

# Intracranial Pediatric Vascular Abnormalities: an Imaging Approach

I.S. Alves, C. Alves, A.P.F. Vieira, C.T. Amancio, D. Delgado, P. Silva, L. Lucato, H.W. Lee, C.C. Leite, and M.G.M. Martin

## CME Credit

The American Society of Neuroradiology (ASNR) is accredited by the Accreditation Council for Continuing Medical Education (ACCME) to provide continuing medical education for physicians. The ASNR designates this journal-based CME activity for a maximum of 1 *AMA PRA Category 1 Credit*<sup>™</sup>. Physicians should claim only the credit commensurate with the extent of their participation in the activity. To claim CME credit for this activity, an online evaluation must be completed and submitted. ASNR members may access this option at no charge (nonmembers must pay a small fee) by visiting <https://www.pathlms.com/asnr>.

## ABSTRACT

Neurovascular disease is less common in children than in adults. Although it corresponds to a small proportion of pediatric pathologies, it represents a clinical challenge because the signs and symptoms are nonspecific, and when the patient presents with stroke or hemorrhage, it is associated with high morbidity and mortality. Intracranial pediatric vascular pathologies can be classified into several types. In this article, we propose a didactic classification based on the presence or absence of shunting and a subclassification of nonshunting arterial diseases according to vessel morphology. From this radiologic perspective, a differential group of pathologies can be included to characterize the specific findings of each disease. In addition to identifying the etiology, gaining insights into the natural evolution of the disease is crucial for the better care of this specific group of patients, which, in some cases, will be evaluated recurrently throughout their lifetimes.

Learning Objective: To describe the main imaging aspects and categorize the pediatric intracranial vascular pathologies.

## INTRODUCTION

Neurovascular disease is uncommon in children. However, it is often associated with high morbidity and mortality rates. Early diagnosis of both ischemic and hemorrhagic strokes can be particularly difficult in children, mostly because of the presence of nonspecific signs and symptoms. In this article, we propose a didactic classification that considers 2 major features: 1) the presence or absence of shunting, and 2) vessel morphology. On the basis of the radiologic perspective, we included several vascular pathologies and grouped them on the basis of the particular findings of each disease for the correct diagnosis.

## CLINICAL MANIFESTATION

Pediatric intracranial vascular pathologies have potentially severe morbidity with variable symptoms that can be associated with hemodynamic flow and the age of manifestation. Hemodynamic status is important during the first 2 years of life when the child can present with cardiac failure due to high-flow arteriovenous shunting (AVS) in early infancy (younger than 3 months of age) and hydrodynamic disorders in infants such as macrocrania and hydrocephalus. Although <15% of infants have seizures as their initial clinical presentation, >70% of them may develop epilepsy later. Seizures in neonates are, in fact due to prior brain

## ABBREVIATION KEY

ASL = arterial spin-labeling  
 AVS = arteriovenous shunting  
 CAMS = cerebrofacial arteriovenous metamerism syndrome  
 CMs = cavernous malformation  
 CVMS = cerebrofacial venous metamerism syndromes  
 dAVS = dural arteriovenous shunting  
 DVA = deep venous anomalies  
 HHT = hereditary hemorrhagic telangiectasia  
 LDS = Loey-Dietz syndrome  
 MMD = Moyamoya disease  
 MPV = median prosencephalic vein  
 NF1 = neurofibromatosis type 1  
 pAVFs = pial AVFs  
 RCVS = reversible cerebral vasoconstriction syndrome  
 SLE = systemic lupus erythematosus  
 VGAM = vein of Galen aneurysmal malformation

Received January 27, 2023; accepted February 16, 2024.

From the Neuroradiology Section, Department of Radiology (I.S.A., A.P.F.V., C.T.A., D.D., H.W.L., C.C.L., M.G.M.M.), Hospital Sirio-Libanes, Sao Paulo, Brazil; Neuroradiology section, Department of Radiology (I.S.A.), Beneficência Portuguesa de São Paulo, São Paulo, Brazil; Neuroradiology Section (C.A.), Department of Radiology, Boston Children's Boston, Massachusetts; Neurology Section (P.S.), Irmandade da Santa Casa de Misericórdia de São Paulo, São Paulo, Brazil; Neuroradiology Section (C.C.L., M.G.M.M., L.L.), Department of Radiology, University of São Paulo, São Paulo, Brazil.

Previously presented as an Education Exhibit at the Annual Meeting of the Annual Meeting of the American Society of Neuroradiology and invited for publication in *Neurographics*.

Please address correspondence to Alves, IS, MD, Department of Radiology, Hospital Sirio-Libanes, Adma Jafet 91, 01308-050, Bela Vista, São Paulo-SP, Brazil; email: [alvesisabelamd@gmail.com](mailto:alvesisabelamd@gmail.com) <http://dx.doi.org/10.3174/ng.2300001>

## Disclosures

Based on the information received from the authors, *Neurographics* has determined that there are no financial disclosures or conflicts of interest to report.

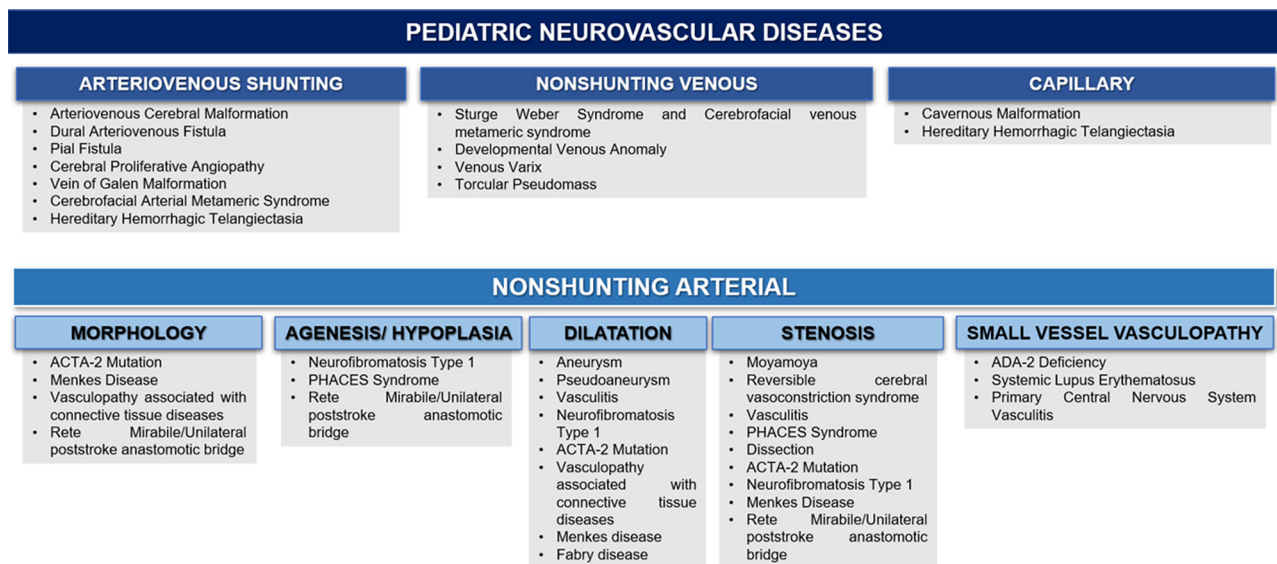


**FIG 1.** To narrow the differential diagnoses of pediatric neurovascular disease, we propose a schematic classification according to the presence or absence of shunting and vessel morphology.

damage. The main clinical concerns are infarction (ischemic or hemorrhagic), hemorrhage (intraparenchymal or subarachnoid), and focal deficits.<sup>1,2</sup>

### CLASSIFICATION OF INTRACRANIAL PEDIATRIC VASCULAR ABNORMALITIES

There are many ways to classify intracranial vascular pathologies, including anatomic aspects, clinical manifestations, etiology, histopathologic and angioarchitectural findings, and hemodynamic status. In this review, we propose a classification of vascular pathology based on imaging, as shown in Fig 1.

#### Arteriovenous Shunting

**Intracranial AVM.** AVMs are defined as vascular anomalies with tangles of abnormal dysplastic blood vessels (nidus) that communicate arteries with veins without intervening capillaries, resulting in a high-flow, low-resistance arteriovenous shunt with an unclear pathogenesis. AVMs may exist in up to 1.4% of the general population and have a similar male/female distribution in the pediatric population. AVMs are usually asymptomatic, with a low rate of hemorrhage (nearly 1% per year) in unruptured cases, and approximately 16% of cases are incidentally found. Symptomatic patients generally present with intracranial hemorrhage (52%), headache without bleeding (20%), and seizures without bleeding (12%). After rupture, the rate of rebleeding increases 5-fold.<sup>3</sup>

The genetic basis of AVMs is still unknown, with pathogenic variants in multiple genes involved in angiogenesis, such as *ALK1*, *RASA1*, *ENG*, *ACVRL1*, *EPHB4*, *SMAD4*, and *KRAS/BRAF*. Two syndromes are associated with AVMs: hereditary hemorrhagic telangiectasia (HHT) and capillary malformation-AVM. The latter is multifocal, usually small, but sometimes large and confluent.<sup>4</sup>

AVMs are usually supratentorial lesions present on CT as hyperdense serpentine vessels or on MRI as a tangle of serpiginous flow voids around an intraparenchymal nidus, with a marked flow enhancement and, usually, minimal mass effect (Fig 2).<sup>4</sup> There are 2 varieties of nidus: 1) The typical glomerular or compact type consists of aberrant vessels without any normal brain tissue interposed, and 2) the proliferative type, which is less common, and is characterized by a normal brain parenchyma scattered throughout the tangle of capillaries. When the last one occurs, proliferative angiopathy or cerebrofacial arteriovenous metameric syndrome (CAMS) needs to be considered in the differential diagnosis.<sup>5</sup> Complications such as edema and hemorrhage may be related to AVMS, and when there is an acute bleeding, phase-contrast MRA with subtraction is frequently helpful in removing the hematoma components.

The imaging modality assessment of AVM includes CTA and DSA, both require contrast media, and MRA, which may be without contrast through the 3D TOF technique or 4D flow MRI (3D phase-contrast), or the dynamic contrast-enhanced sequence (time-resolved imaging of contrast kinetics [TRICKS]/time-resolved imaging with stochastic trajectories [TWIST]).<sup>6</sup>

In angiographic studies, AVMs have 3 main components: enlarged feeding arteries, nidus (“honeycomb” vascular channels), and a dilated early draining vein. The AVM nidus can change with time, and the intranidal “aneurysm” represents an angioarchitectural weak point and should be actively sought. Because AVMs usually present as a nontraumatic intracranial hemorrhage in a toddler, angiography examinations should be promptly performed.<sup>4</sup>

Perfusion analysis can be performed using whole-brain perfusion studies. Kim and Krings,<sup>7</sup> 2011, described 3 distinct patterns of extranidal and perinidal brain parenchymal

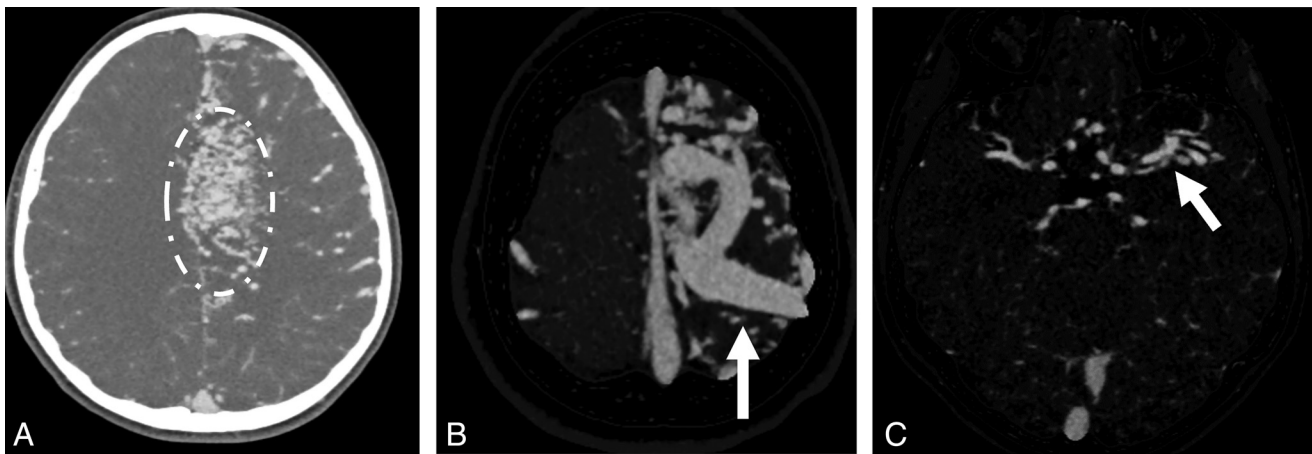


**FIG 2. AVM.** Arterial CTA (A) shows an enhancing vascular lesion in the left parasagittal frontal lobe. Dynamic time-resolved imaging of contrast kinetics (TRICKS) MRA (B) and Subtraction (C) shows a superficial cortical vein drainage (B) with left MCA ectasia (C).

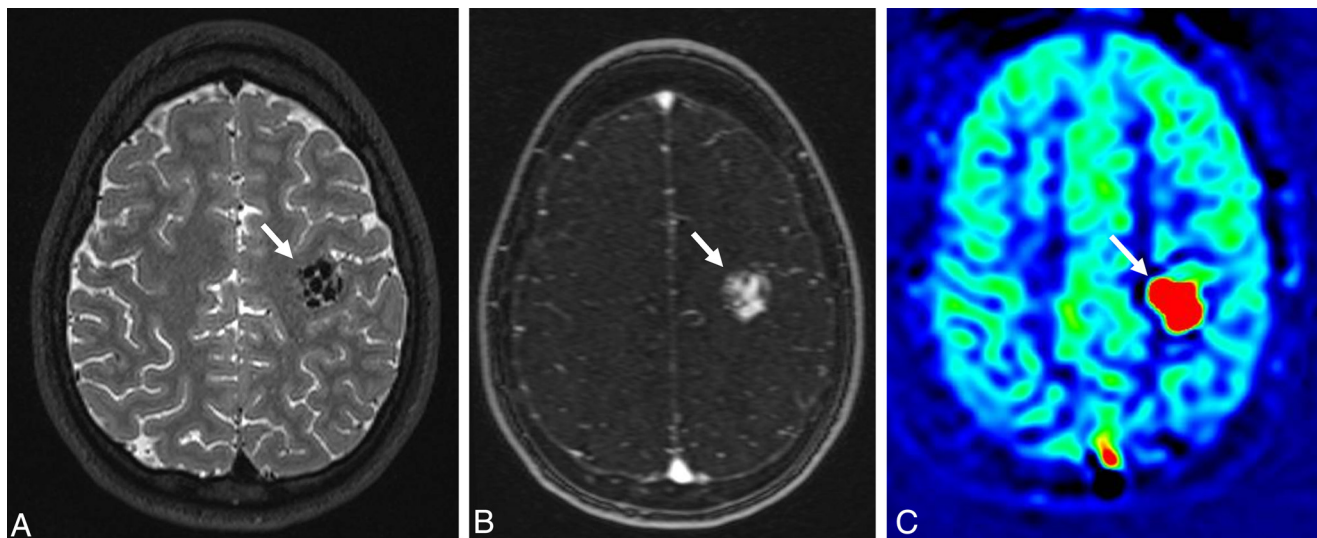


**FIG 3. AVM.** Axial T2-weighted MRI (A) demonstrates multiple vascular structures at the left frontoparietal junction, with a superficial nidus visible on dynamic time-resolved imaging of contrast kinetics (TRICKS) MRA (B), and high CBF on ASL (C).

perfusion: 1) functional steal clinically present as seizure, characterized by decreased CBF, CBV, and MTT; 2) ischemic steal, characterized by decreased CBF and CBV and increased MTT presenting as a focal neurologic deficit; and 3) venous congestion, characterized by increased CBV and MTT with different clinical symptoms such as neurologic deficit, seizure, hemorrhage, and chemosis.<sup>7</sup> After treatment, brain perfusion follow-up images, particularly ASL, can help identify and quantify the remaining high-flow intranidal areas (Fig 3).<sup>8,9</sup>

The AVM classification and grading are usually based on the Spetzler-Martin scale (Table 1), which evaluates the size of the nidus, location, and venous drainage with a score ranging from 1 to 5. A high score correlates with a high risk of open surgery. Grade 6 describes inoperable AVMs.<sup>10</sup> The treatment for AVMs includes clinical management, endovascular embolization, microsurgical resection, stereotactic radiosurgery, or multimodal therapy.<sup>3</sup>

**Table 1: Spetzler-Martin Scale<sup>a</sup>**

Size of Nidus	Eloquent Area	Venous Drainage
Small (<3 cm) = 1	Noneloquent = 0	Superficial veins only = 0
Medium (3–6 cm) = 2	Eloquent = 1	Deep veins = 1
Large (>6 cm) = 3		

<sup>a</sup>Eloquent brain: sensorimotor, language, visual cortex, hypothalamus, thalamus, brain stem, cerebellar nuclei, or regions immediately adjacent to these structures

**Dural AVF.** A dural AVF is an extremely rare vascular pediatric malformation and can be divided into 3 types: dural sinus malformation with dural arteriovenous shunting (dAVS), infantile dAVS, and adult-type AVS. Dural sinus malformation presents as anatomically focal dilated and bulging dural sinus ectasia. It has 2 types: 1) in the midline involving the confluence of sinuses and adjacent sinuses; and 2) off-midline involving the jugular bulb, which represents a petromastoid-sigmoid sinus high-flow AVF with preserved cerebral venous drainage. The most significant prognostic

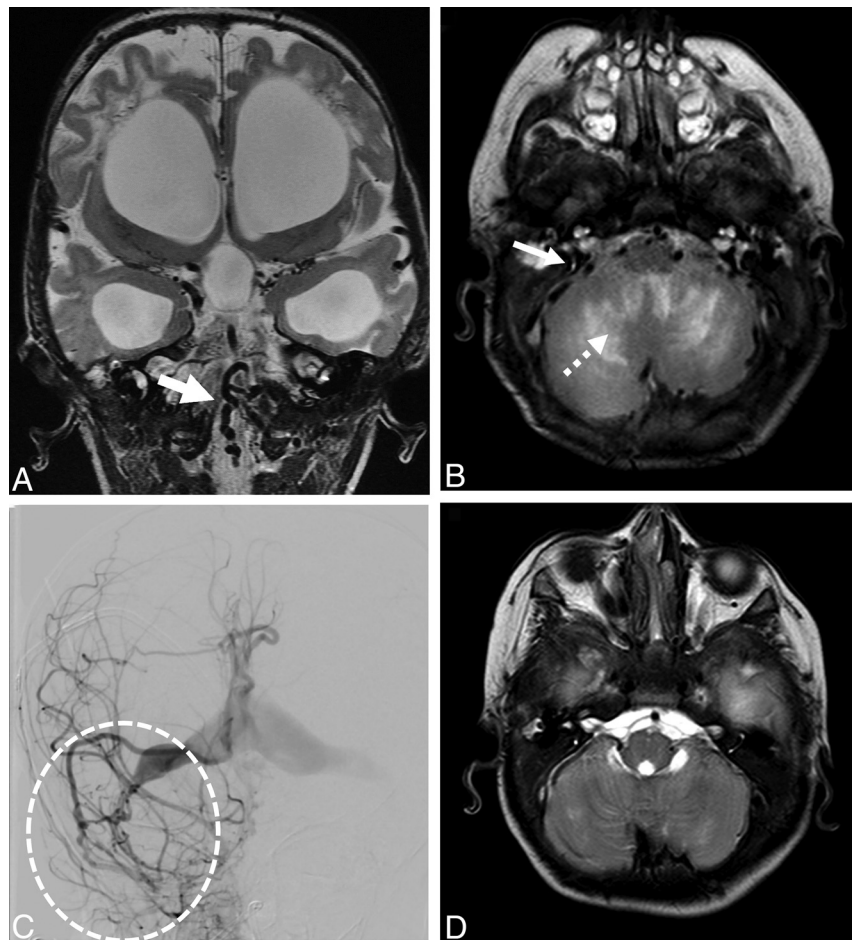


**FIG 4. Congenital dural fistula. A,** Coronal T2WI MRI shows tortuous vessels with flow voids. **B,** Axial FLAIR shows cerebellar white matter edema due to venous congestion (*dotted arrow*) with dilated vessels in the subarachnoid space (*arrow*). Angiography (**C**) shows a complex multiple-feeding artery AVF with stenosis / occlusion of the jugular bulb (circle). Note the resolution of cerebellar white matter edema after embolization (**D**).

markers that should be evaluated with MRI are the involvement of the torcula, the condition of the jugular bulb, and the signs of cavernous sinus recruitment.<sup>2</sup> Early dAVS correction and preservation of the impaired venous outflow through anticoagulation with low-molecular-weight heparin are the treatment objectives.<sup>11</sup>

Infantile dAVS is the most frequent type in childhood and is characterized by dural high- and low-flow shunts, often multifocal, draining into an enlarged sinus that remains patent for a long time, lacks progressive neurologic deficits, and is usually diagnosed in older children. Arterial embolization is usually partial, and recurrence leads to a poor prognosis.<sup>2,12</sup>

The probable pathogenic origin of adult-type AVS (Fig 4) is a focal angiogenic response to venous thrombosis. The cavernous sinus is the most common location, and the sigmoid sinus is rarely involved. It has an often favorable evolution because spontaneous regression often occurs.<sup>12</sup>

**Pial AVF.** Pial AVFs (pAVFs) are rare but clinically relevant vascular lesions of the CNS characterized by direct arterial connections to a pial venous channel without an intervening nidus. The incidence of these lesions ranges from 3% to

4.8%.<sup>13</sup> Although pAVFs are frequently thought of as congenital lesions, a few uncommon examples of acquired pAVFs have been reported in the literature.<sup>14</sup> Genetic studies on pAVFs are limited. The specific genes associated with the development of pAVFs have not been extensively characterized; however, they have been reported to be associated with hereditary hemorrhagic telangiectasia (HTT) and capillary malformation-AVM. Clinical manifestations can include high-output cardiac failure, macrocrania, neurodevelopmental delay, seizures, venous infarctions caused by venous stenosis, or hemorrhage due to venous thrombosis, depending on the patient's age. Depending on the clinical and angiographic criteria, pAVFs can be treated with microsurgery, endovascular procedures, or a combination of both.<sup>15,16</sup>

**Vein of Galen Aneurysmal Malformation.** Vein of Galen aneurysmal malformation (VGAM) is characterized by the failure of regression of the median prosencephalic vein (MPV, or vein of Markowski) around the 11th week of gestation, along with an MPV arteriovenous fistula (AVF) involving deep choroidal arteries. This condition is usually associated with persistence of the falcine sinus and absence of the straight sinus.<sup>17</sup> Recent studies have identified a

genetic background in VGAM patients, including mutations in RASA1 (RAS p21 Protein Activator 1) and EPHB4 (Ephrin type-B receptor 4), which encode proteins involved in vascular development. VGAM is the most common cause of extracardiac high-output cardiac failure in neonates and is classified into two types according to the Lasjaunias system: mural and choroidal (Fig 5). The mural type VGAM is a direct AVF, characterized by a single or multiple arterial fistulas at the inferolateral margin of the MPV, while the choroidal type is a more primitive and severe condition, presenting as a complex vascular network with small, nidus-like vessels carrying arterial flow into the anterior aspect of the MPV (Fig 6). The MPV typically drains into the straight sinus (if present) and subsequently through the transverse and sigmoid sinuses. However, alternative drainage routes through the cavernous sinus may develop in cases of sigmoid sinus or jugular bulb occlusion.<sup>18</sup> The venous system should be carefully assessed, particularly looking for internal cerebral vein drainage into the VGAM, jugular bulb or sigmoid sinus stenosis, and the superior sagittal sinus (SSS) and falcine/straight sinus diameter. SSS stenosis and dilatation of the falcine or straight sinus are associated with poor prognosis.<sup>19</sup> Some studies provide quantification of sinus stenosis and dilatation: the SSS index is calculated as the width of the flow void in the sagittal sinus on coronal T2SE divided by the biparietal diameter, multiplied by 100. An SSS index of  $\leq 3$  at onset is associated with poor clinical outcomes.<sup>20</sup> Additionally, a straight or falcine sinus diameter greater than 6.2 mm in neonates and 5.2 mm in fetuses (measured at its narrowest mediolateral point in the craniocaudal axis) is also associated with poor prognosis, indicating the need for earlier intervention.<sup>19</sup> Other prognostic features that should be assessed include ventricular dimensions and the integrity of the brain parenchyma, with particular attention to ischemic infarcts, calcifications secondary to venous congestion, and cavitations in the white matter. Additionally, associated findings to look for include MCA pseudofeeders, which are enlarged branches of the M2 or M3 segments of the MCA that supply the brain parenchyma but do not feed the AVM. This finding suggests impaired cerebral blood flow and is critical for prognostic evaluation. Occasionally, a hair-like collateral network of vessels may develop in the thalamus, resembling a “true” AVM. This phenomenon, known as fine, vascular network formation (FVNF), is acquired and reversible, typically resolving after treatment completion, and its resolution correlates with the closure of the vein.<sup>21</sup> The urgency of treatment depends on clinical conditions, as well as cardiothoracic and intracranial parameters. Management typically involves surgery, endovascular procedures (most commonly transarterial embolization), or gamma knife treatment. If left untreated, VGAMs usually lead to chronic venous ischemia, presenting as subcortical white matter calcification, subependymal atrophy, and ventricular dilation due to either hydrocephalus or parenchymal volume loss.<sup>22</sup>

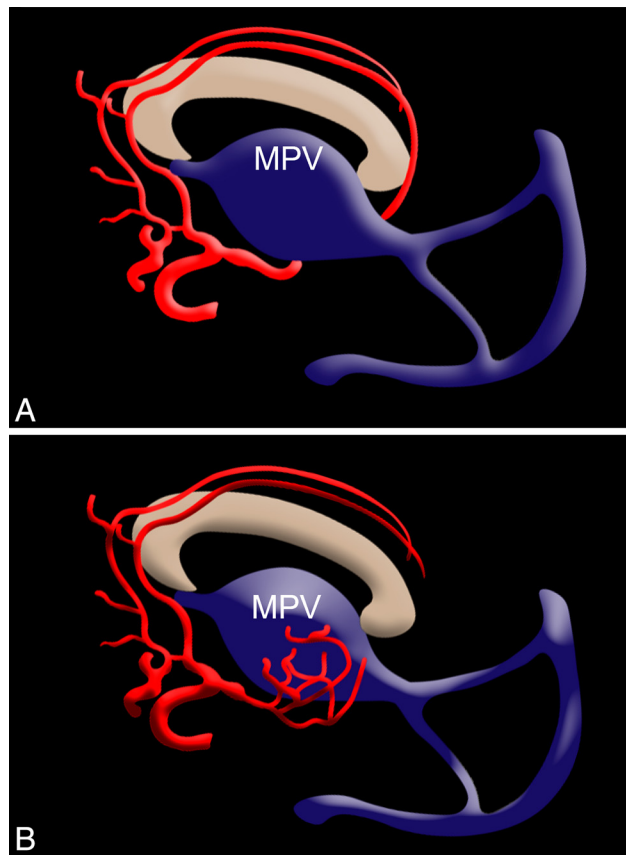
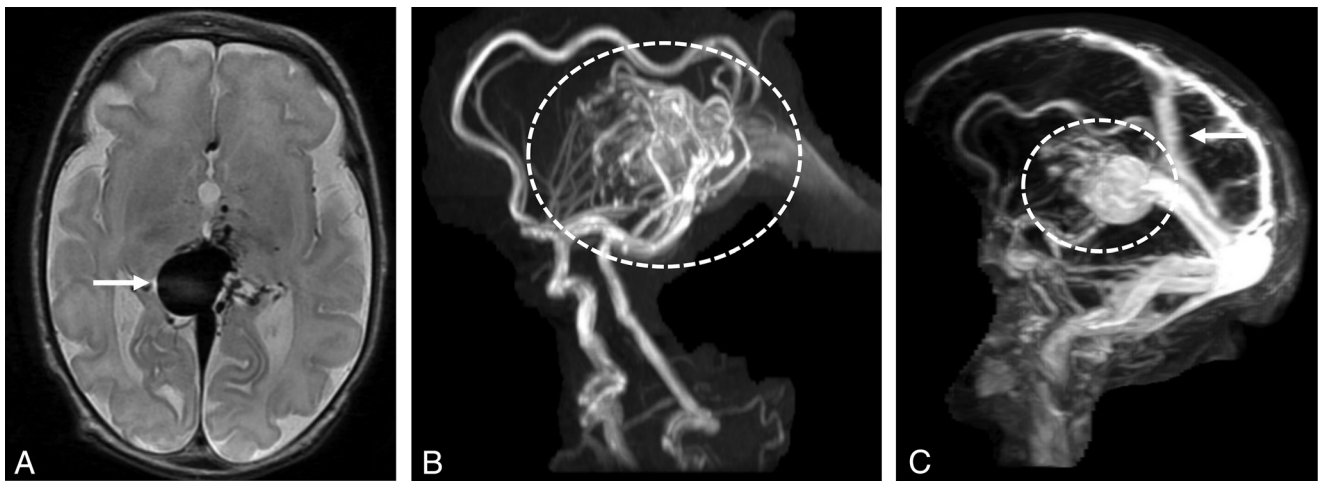


FIG 5. Drawing of VGAM subtypes: mural-type (A) and choroidal-type (B).

**Cerebral Proliferative Angiopathy.** Cerebral proliferative angiopathy is a separate entity from AVM, being rare in pediatric patients. It is characterized by a diffuse and dense vascular network with intermingled normal brain parenchyma and the absence of dominant feeders. The term proliferative is related to new blood vessel formation in this disease, which is presumably induced as a partial response to cortical ischemia. On imaging, cerebral proliferative angiopathy often appears as a tiny and tortuous blood vessel network among healthy brain tissues and may be linked to hemorrhage, calcifications, or perilesional edema (Fig 7). The key to distinguishing this illness from traditional brain AVMs is the absence of obvious early venous drainage on dynamic imaging.<sup>5</sup> Treatment involves a multidisciplinary approach that aims to enhance blood supply to healthy brain tissue, manage symptoms, and prevent complications.<sup>23</sup>

**Metameric Vascular Syndromes.** These metameric vascular diseases are characterized by segmental vascular anomalies involving the spine and craniofacial region. They can be divided phenotypically as CAMS, cerebrofacial venous metameric syndromes (CVMS), spinal arteriovenous metameric syndromes, and some authors also includes PHACES syndrome (P: posterior fossa malformations, H: hemangiomas, A: arterial anomalies, C: coarctation of the aorta



**FIG 6. VGAM.** Axial T2WI MRI (A) shows a markedly enlarged median prosencephalic vein of Markowsky, characteristic of a Galen vein aneurysmal malformation. Oblique sagittal arterial (B) and venous (C) MRAs show multiple enlarged arterial branches coalescing on the dilated recipient vein (circle) and persistence of the falcine sinus. (arrow in C).

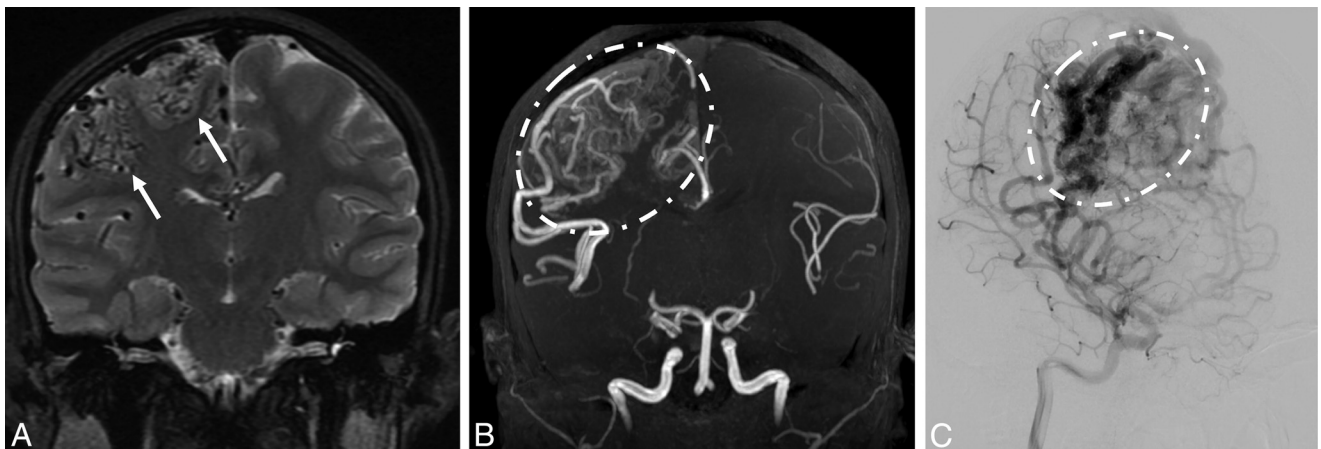


**FIG 7. Cerebral proliferative angiopathy.** Coronal T2WI MRI (A) demonstrates intraparenchymal dilated flow voids involving the right frontoparietal lobes (arrows). Coronal MRA (B) and oblique coronal angiography (C) highlight the absence of early venous drainage and a diffuse nidus with mild enlargement of the feeder arteries (circles).

and cardiac anomalies, E: eye [ocular] anomalies, S: sternal clefting and/or supraumbilical raphe).<sup>24</sup> Cerebrofacial vascular metamerism syndrome has been related to postzygotic (mosaic) activating pathogenic variants in the PI3K–RAS–MAPK pathway, especially in the PIK3CA and TEK receptor tyrosine kinase (TEK) gene pathways.<sup>25,26</sup> CVMS and Sturge-Weber will be described in nonshunting venous diseases.

CAMS, is characterized by the presence of multiple AVMs in the brain parenchyma and facial regions (Fig 8), including Wyburn-Mason syndrome or Bonnet-Dechaume-Blanc disease, which primarily involve the brain, orbits, and facial structures. CAMS has 3 classic subtypes that may overlap, resulting in mixed phenotypes:<sup>27</sup>

- CAMS type 1 includes the medial prosencephalon and AVMs in the corpus callosum, hypothalamus (hypophys), and nose

- CAMS type 2 affects the lateral prosencephalon, with AVMs in the occipital lobe and optic tract, including the thalamus, retina, and maxilla
- CAMS type 3 involves the rhombencephalon, with AVMs in the cerebellum, pons, and mandible.

The diagnosis relies on neuroimaging, initially, MRI, followed by DSA, which is essential to confirm the diagnosis and evaluate the angioarchitecture and AVM hemodynamics. The treatment is variable and should be evaluated individually.<sup>2,27</sup>

#### HHT

Hereditary hemorrhagic telangiectasia or Osler-Weber-Rendu is an autosomal disorder with prevalence of 1:5000 people in North America and is the most classic syndrome related to multiple brain AVMs. The prevalence of HHT in patients with brain AVMs is approximately 2%–3%, and

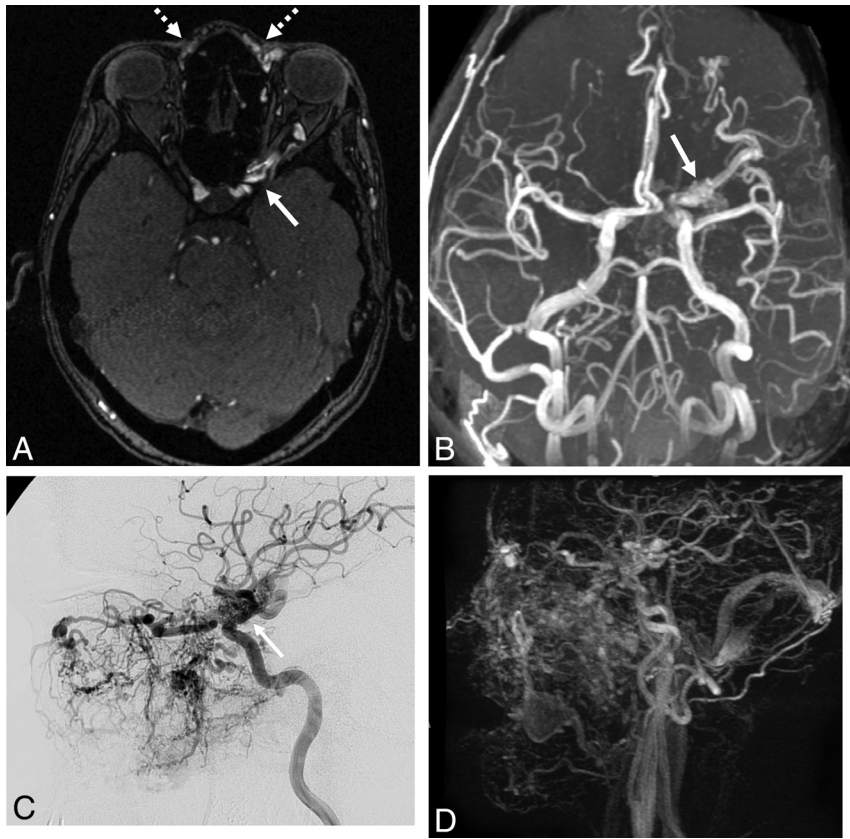


**FIG 8. CAMS.** Axial arterial MRA (A), axial oblique arterial MRA with MIP (B), and sagittal oblique DSA (C) show multiple arterial branches adjacent to left ophthalmic artery involving the left optic canal and nerve (arrow), left orbit medial canthus, and bilateral nasal soft tissue (dotted arrow). MIP sagittal venous MRA (D) shows a complex facial arteriovenous malformation.

among patients with HHT, 5%–23% may show brain AVMs. HHT has a multisystemic involvement with clinical diagnosis based on the presence of the following criteria: recurrent spontaneous epistaxis, multiple mucocutaneous telangiectasia (including oral cavity, lips, fingers, and nose), visceral AVMs, and a first-degree relative with HHT. The presence of 3 of 4 criteria is a “definitive” diagnosis, while “suspected” is the presence of 2 criteria and “unlikely” is when there is only 1 criterion present. The genotype of HHT is caused by a mutation in some different genes, such as endoglin or *ENG* for HHT type 1, the HHT type 2 is related to activin A receptor-type II-like 1 (*ACVRL1*) or *ALK1*. Myhre syndrome, a juvenile polyposis HHT, is related to *SMAD4* mutation, and HHT type 5 is associated with growth differentiation factor 2, bone morphogenic protein 9. Types 3 and 4 are clinically defined, but the genetic cause remains unknown.<sup>28</sup> The 3 main types of vascular CNS abnormalities are AVMs, Pial AVFs, and capillary malformation, which are usually located in the supratentorial compartment and are superficial. Brain AVMs tend to be small, and when <1 cm, they are called “micro-AVMs.”

These are the most common HHT-related CNS vascular malformations. Other vascular CNS findings include developmental venous anomalies, VGAMs, and mixed lesions. Arterial aneurysms (Fig 9) have also been described in up to 10% and may be associated with older age, the presence of unrelated AVMs, and the presence of the



**FIG 9. HHT.** 3D axial volume-rendering reconstruction arterial CTA shows a saccular aneurysm in the left MCA bifurcation (arrow).

*ACVRL1* mutation.<sup>29</sup> These lesions may rupture and bleed. Therefore, screening is important, though no consensus has been reached in the literature. Some centers recommend, for individuals with definitive HHT, screening with MRI in the first 6 months of life or at the time of diagnosis, followed by imaging every 5 years until 25 years of age, whereas others perform imaging during childhood and later in adulthood.<sup>28,30</sup>

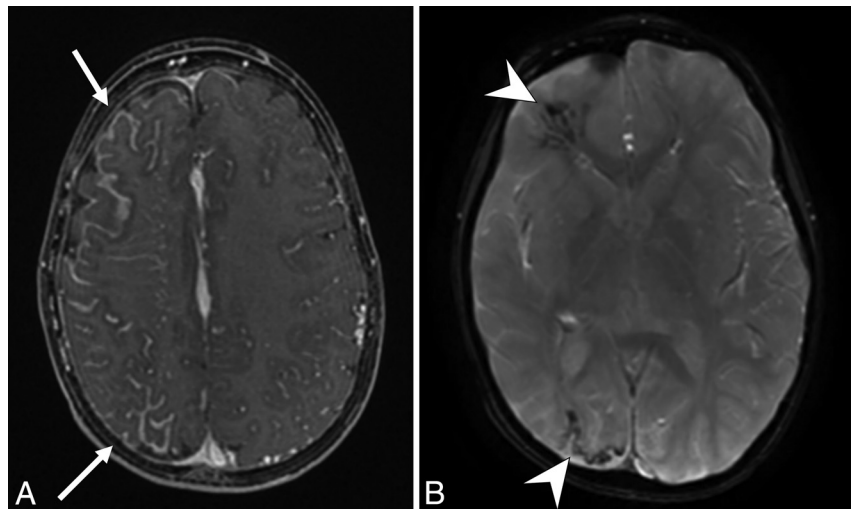


**FIG 10. Sturge-Weber syndrome.** Axial T1 contrast-enhanced MRI (A) shows prominent leptomeningeal enhancement in the right cerebral hemisphere (arrows) with parenchymal volume loss. Axial T2 gradient-recalled echo (B) shows subcortical calcifications (arrowhead).

### Nonshunting Venous

**Sturge-Weber Syndrome and CVMS.** CVMS includes the spectrum of cervicofacial venous malformations as a part of metameric slow-flow vascular malformations with the presence of deep venous anomalies (DVA) and/or dural venous sinus anomalies, such as dural ectasia and persistent falcine sinus, and/or the presence of cavernous malformations (CMs). CVMS can be clinically suspected on the basis of the presence of a large facial port wine stain or extensive hemifacial venous vascular malformations. DVAs are usually present in the same metamere in nearly 75% of cases and are ipsilateral in approximately 80% of cases in a large series study. The classic form of CVMS is Sturge-Weber syndrome, or encephalotrigeminal angiomasia (Fig 10), which has been linked to a nucleotide transition in *GNAQ* on chromosome 9q21 and is characterized by facial port wine staining associated with cortical atrophy/calcifications, volume loss, and leptomeningeal angiomasia on the same side as the facial stain.<sup>31,32</sup>

**DVA.** DVAs are common incidental findings in neuroimaging studies, representing an anatomic venous variation in the CNS. The main DVAs are sporadic, typically isolated, and not associated with underlying genetic mutations; however, they can be found in a subset of genetic-related cavernous malformations or associated with other vascular malformations, such as venous malformations of the face, head, and neck. DVAs appear as a radial arrangement of small veins draining into a large central vein with a typical “caput medusae” appearance.<sup>33</sup> In a review of neonatal DVAs, this venous variant was detected in approximately 2% of cases; one-third of neonatal DVAs may be complicated by parenchymal abnormalities, including hemorrhage, infarction, and gliosis; The multiplicity of DVAs (presence of  $\geq 1$ ) was significantly associated with complications. However, in most cases, neurologic outcomes are favorable and self-limiting.<sup>34</sup>

**Venous Varix.** Venous varix, also known as cerebral venous aneurysms or cerebral varix, is an uncommon intracranial vascular abnormality, and the prevalence and clinical significance of these conditions are not well-established. This condition is usually related to other vascular malformations such as dural AVFs and is rarely found alone. On imaging, clearly defined spindle-shaped focal venous dilation with a distinct boundary and smooth contours may be associated with bone erosion (Fig 11). This appearance can mimic a meningioma on CT and MRI because of its cortical location; however, bone erosion may help in the differential diagnosis. DSA and MR venography may aid in making a definitive diagnosis and revealing the venous anatomy of the varix.<sup>35</sup>

### Torcular pseudomass

The torcular pseudomass is characterized by redundant extra-axial soft tissue between the torcular herophili and occipital squama, with a frequency estimated around 12.7%. On imaging, it presents as a mass isointense on T1WI and hyperintense on T2WI to the cerebral cortex, high signal on DWI/ADC map, and may show contrast enhancement (Fig 12). Torcular pseudomass is an incidental finding that should be physiologically related to the postnatal period. It is not associated with factors related to delivery and usually shows complete resolution during follow-up, though sometimes it may be found in older individuals.<sup>36</sup>

### Capillary

**CMs.** CMs, the so-called cavernomas, are the most common angiographically “occult” vascular malformations and are classified as slow-flow venous malformations composed of sponge-like clusters of hyalinized dilated thin-walled capillaries with surrounding hemosiderin (Fig 13). They are usually sporadic but can be genetically determined. When hereditary, they are autosomal dominant with variable penetrance, with usually multiple CMs and associated mutations in *CCM1*

(*KRIT1*), *CCM2* (*MGC4607* or malcaverin), or *CCM3* (*PDCD10* or programmed cell death 10) protein-encoding genes, indicating that *CCM1* is associated with more lesions throughout life, while *CCM3* is associated with a higher risk of hemorrhage. The main differential diagnosis of multiple familial CMs is related to postradiotherapy CMs, with <10% of multiple CMs related to sporadic cases.<sup>37</sup> On CT, they usually appear as hyperdense nodular lesions, with normal findings on MRA and DSA, while on MRI, they have different forms of presentation described by Zabramski et al.<sup>38</sup>

- Type 1 (subacute hemorrhage) with a T1-hyperintense core and T2-hyper- or hypointense core surrounded by a hypointense rim



**FIG 11. Venous varix.** Coronal T1 contrast-enhanced MRI shows fusiform cortical venous varix (arrow).

- Type 2 (classic popcorn appearance) with a T1 and T2 mixed-signal core with a surrounding T2 hypointense rim
- Type 3 (chronic hemorrhage) with a T1 iso- or hypointense core and a T2-hypointense rim and T2\* low-signal rim with blooming
- Type 4 is poorly seen on T1 and T2, presenting as a punctate hypointense lesion on T2\*.

The most commonly associated abnormalities are DVA, superficial siderosis, T2/FLAIR white matter hyperintensity, and cutaneous abnormalities such as café au lait spots and hyperkeratotic capillary-venous malformations. Incidental CMs have an overall annual bleeding rate of approximately 0.5%–1%, whereas previous bleeding lesions have a rate of >18% for hemorrhage recurrence within 3 years. After bleeding, to better visualize the CMs images, follow-up should be performed after clot re-absorption 4–6 weeks later. Management can be performed through clinical observation or surgical resection. Imaging screening should be considered for first-degree relatives of patients with multiple or familial CMs.<sup>3</sup>

## NONSHUNTING ARTERIAL

### Morphology

**Phenotype ACTA2 Mutation** The Arg179His ACTA2 mutation is a cause of multisystem smooth-muscle involvement, classified as a prototype example of nonatherosclerotic cerebral arteriopathies, and is not a variant of Moyamoya disease. Arteriopathy is characterized by a straight course of the cerebral arteries (“broomstick appearance”), proximal internal carotid artery dilation and stenosis or occlusion of the distal ICAs without Moyamoya-like collaterals. In a review of the ACTA2 phenotype in the brain parenchyma, all patients presented with a V-shaped hypoplastic corpus callosum, abnormal radial gyration of the frontal lobes, a deficient anterior cingulate gyrus, and a variable degree of fornix horizontal orientation and thickening. Ninety-three

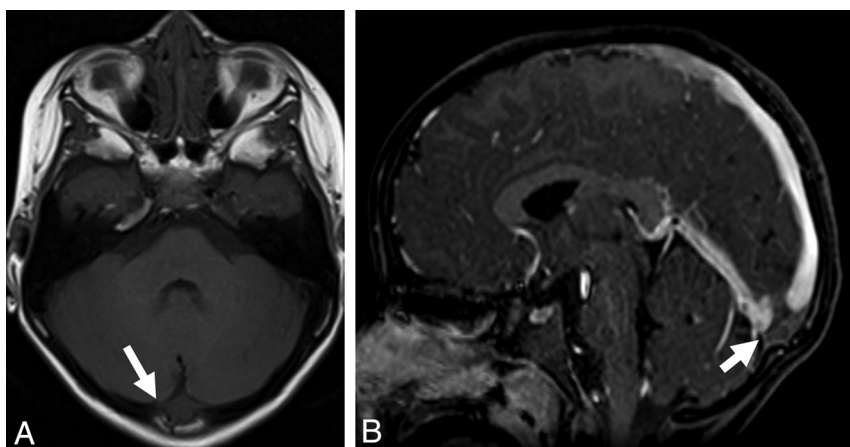


**FIG 12. Torcular pseudomass.** Axial T1WI MRI (A) shows a redundant soft tissue between the venous sinuses confluence and the occipital squama posterior to the Herophili torcula (arrow). The sagittal T1 contrast-enhanced MRI (B) shows that the tissue has a slight enhancement (arrow).

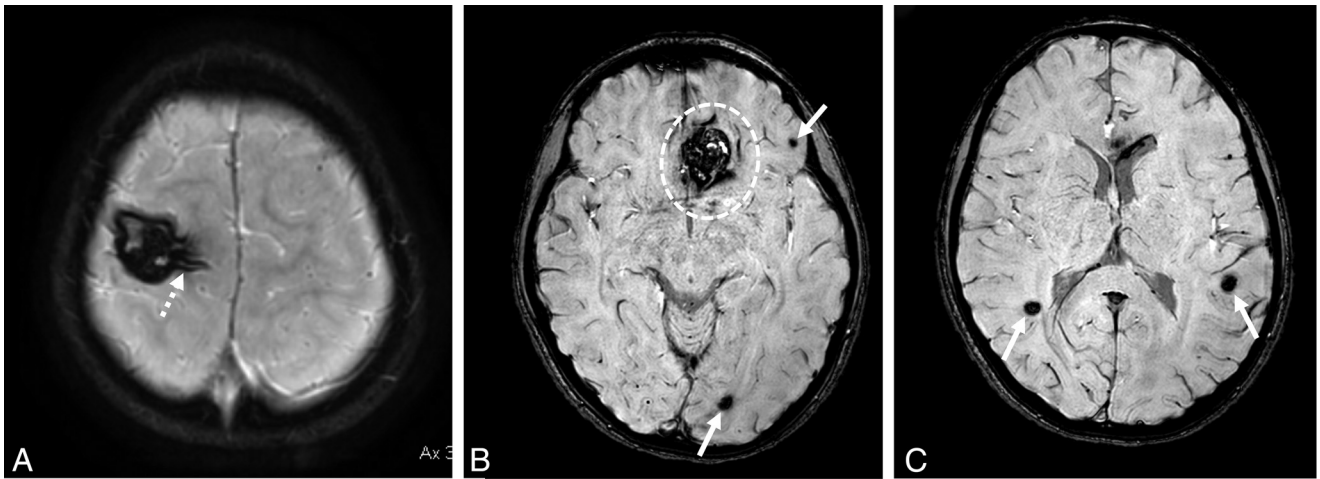


**FIG 13. Cavernous malformation.** Axial SWI shows multiple CMs (arrow) with blooming effect (circle) and adjacent superficial siderosis (dotted arrow).

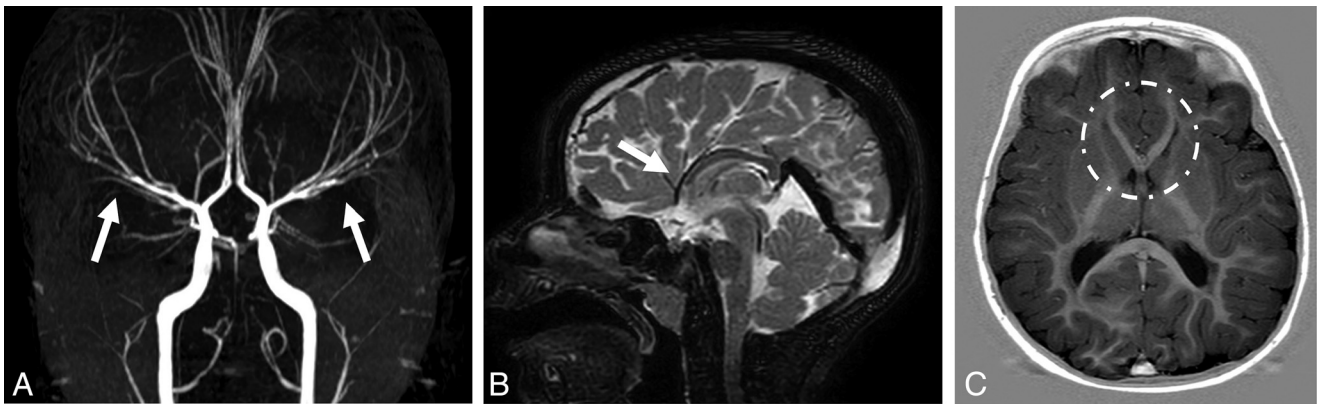


**FIG 14. ACTA-2 mutation.** A, Coronal MIP MRA shows dilation of the proximal ICAs, narrowing the distal ICAs, and straight “broomstick-like” arteries of the circle of Willis (arrow). Sagittal T2WI (B) shows typical hypoplasia and bending of the anterior corpus callosum associated with a deficient anterior cingulate gyrus (arrow). Axial T1WI (C) demonstrates the characteristic V-shaped anterior corpus callosum (white circle).

percent had the “twin peaks pons sign” characterized by reduction of the anterior-posterior diameter on the midline and an impression of the basilar artery on the anterior surface with the consequent presence of 2 symmetric prominences resembling twin mountains and also multiple indentations on the surface of the pons in parasagittal view, probably due to the compression of straightened pontine arterial branches. Eighty-five percent presented with “squeezing” appearance of the midbrain cerebral peduncles (Fig 14).<sup>39</sup>

#### **Menkes disease**

Menkes disease, also known as trichopoliodystrophy or kinky hair kinky vessel syndrome, is a rare X-linked recessive disorder that affects males and is caused by a mutation in the *ATP7A* gene (Xq13.2-q13.3) that results in derangement in copper absorption and cellular metabolism. The main clinical findings were early growth failure, classic kinky hair (*pili torti*), seizures, developmental delay, and urinary bladder diverticula. The CNS findings associated are the following: 1) intracranial vessel tortuosity that

increases during follow-up without arterial ectasia or stenosis; and 2) white matter lesions can be divided into 3 subtypes: a) tumefactive lesions, which are vasogenic edema that spares the cortex with a mild mass effect mostly involving the temporal lobe and do not have a vascular/ischemic pathogenesis and may also be reversible; b) DWI-hyperintense centrum semiovale lesions that have an imaging appearance of cytotoxic-like lesions that may show a persistent DWI restriction on follow-up; c) the focal nontumefactive white matter lesion that has a frequency above 40%; d) abnormal myelination, though most children have normal myelination at birth (On follow-up, abnormal supratentorial myelination is usually reported.); and e) subdural collections that are a relatively common finding (Fig 15).<sup>40,41</sup>

#### **Vasculopathy Associated with Connective Tissue Disorder**

Connective tissue disorders are caused by defects that impair connective tissue, resulting in weakened vessel walls,

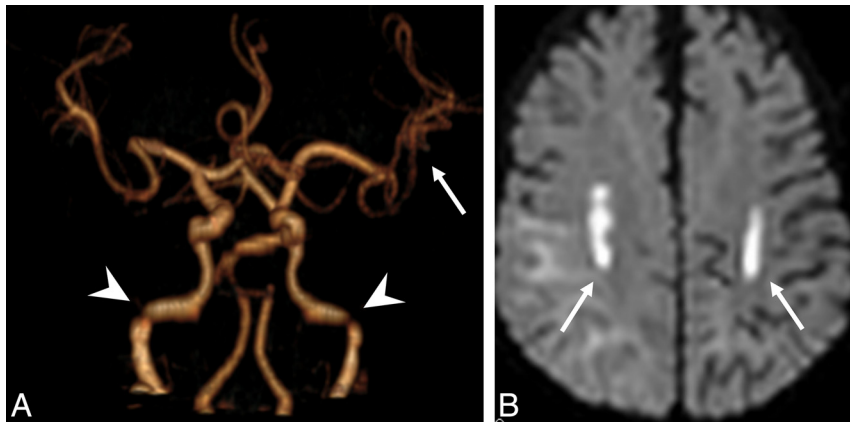


**FIG 15. Menkes disease.** Intracranial MRA 3D reconstruction (A) shows tortuous arteries (arrows) with focal stenosis (arrowhead). Axial DWI (B) shows centromedian areas of infarction (arrows). Courtesy of Dr. Cecilia Purcellas, Montevideo, Uruguay.

including Marfan syndrome, Ehlers-Danlos syndrome type IV, and Loeys-Dietz syndrome (LDS), which are autosomal dominant but may occur as sporadic mutations. Marfan syndrome is caused by a defect in the fibrillin-1 gene familial disorder of connective tissue with variable phenotypic expression, especially musculoskeletal, ocular, and vascular manifestations, including arterial tortuosity and intracranial aneurysms.<sup>42</sup> Ehlers-Danlos syndrome (Fig 16) has various phenotypes (multiple syndromes), highlighting type IV caused by a defect in the gene that encodes for type III collagen, *COL3A1*, which may show arterial rupture, dissections, aneurysms, and cavernous-carotid fistulas.<sup>43</sup> LDS is caused by heterozygous mutations in the genes encoding transforming growth factor B receptor traced to chromosomes 9q33 and 3p24, with a clinical triad of hypertelorism, arterial tortuosity, aneurysms, or dissections, and bifid uvula or cleft palate.<sup>44</sup> The measurement of tortuosity indexes of intracranial arterial segments on a 3D volume-rendered angiogram, specially the vertebrobasilar system, may help to predict LDS and, in some cases, differentiate LDS from Marfan syndrome.<sup>45</sup>

### **Agenesis/Hypoplasia**

**Neurofibromatosis Type 1.** Neurofibromatosis type I (NF1), or von Recklinghausen disease, is a neurocutaneous autosomal dominant disorder that affects 1:3000– 5000 individuals. The *NF1* gene locus is located on the long arm of chromosome 17, which produces neurofibromin that acts as a tumor suppressor of the Ras/MAPK pathway and is also classified as a RASopathy. On imaging, it is characterized by hypoplastic or aplastic carotid canals, vascular dysplasia, nonenhancing T2/FLAIR signal white matter abnormalities, soft-tissue plexiform neurofibromas, primarily optic pathway gliomas, skeletal dysplastic lesions, and skin café au lait spots. In a review of the general vascular abnormalities of NF1, the most common abnormalities were aneurysm, arterial stenosis, AVM, and arterial compression, or invasion by neural tumors (Fig 17). Vascular

abnormalities in pediatric patients are around 18%, with the Moyamoya pattern being the most common vascular abnormality.<sup>46,47</sup>

### **PHACES syndrome**

It is a phacomatosis of unknown etiology that represents an acronym for posterior fossa malformation (P), hemangioma (H), arterial cerebrovascular anomalies (A), coarctation of the aorta and cardiac defects (C), eye abnormalities (E), and sternal clefting or supraumbilical raphe (S). Cerebral and cervical arterial anomalies are the most common extracutaneous abnormalities, characterized by vascular dysplasia, aberrant origin or course, absence or agenesis, hypoplasia, stenosis, occlusion, persistence of fetal vessels, and presence of saccular aneurysms (Fig 18).<sup>48</sup> According to brain MRA findings, the risk of a cerebrovascular accident can be graded as the following: 1) low: findings without or with a very low clinical impact on patient outcome, such as primitive embryonic circulation or an anomalous course; 2) intermediate: nonstenotic dysgenesis, narrowing or occlusion without hemodynamic risk in proximal arteries of the circle of Willis; and 3) high: significant narrowing (>25%) or occlusion of main cerebral vessels within or above the circle of Willis, which results in an “isolated” circulation or tandem or multiple arterial stenoses associated with complex blood flow leading to a possible reduction on cerebral perfusion. Neurologic and cognitive deficits are usually associated with cerebrovascular anomalies and are closely associated with morbidity in these patients, though there are few reports on their long-term outcomes.<sup>49</sup>

### **Rete mirabile anomaly**

The Rete mirabile anomaly or twig-like MCA (Fig 19) is characterized by a net of vascular channels instead of a M1 trunk of the middle cerebral artery. It is hypothesized as an absent MCA with a persistent primitive plexus of the MCA, with no steno-occlusive disease of the distal ICA (to differentiate from MoyaMoya pattern). There is some controversy, though, as a unilateral pattern of anastomotic bridges has been described to evolve after unilateral arterial

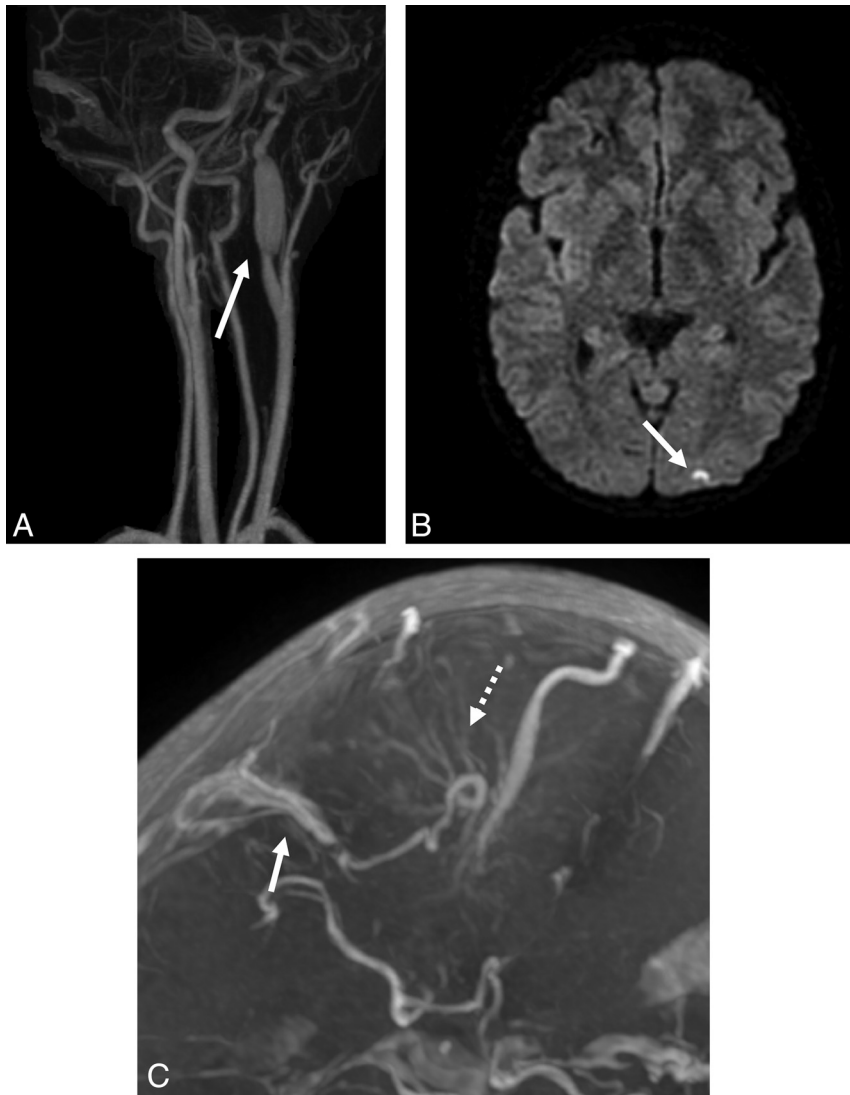


**FIG 16.** Vasculopathy secondary to a connective tissue disorder (Ehlers-Danlos). Oblique sagittal arterial cervical MIP MRA (A) shows a pseudoaneurysm related to cervical dissection (*arrow*). Axial DWI (B) shows a focal cerebral infarction in the left occipital lobe, and sagittal intracranial MRA MIP (C) shows a microfistula (*arrow*) and developmental venous anomalies (*dotted arrow*).

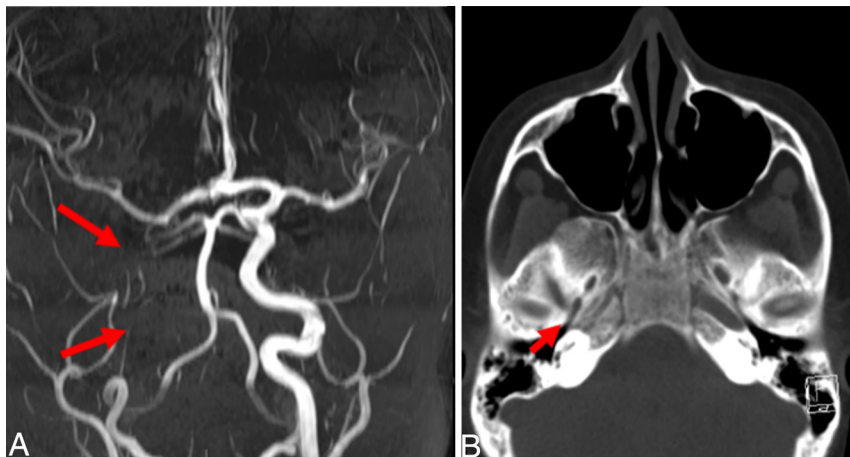


**FIG 17.** NF1. Coronal MIP MRA (A) shows agenesis of the right ICA (*arrow*). Axial CT scan bone window (B) shows a remarkably reduced carotid canal (*arrow*).

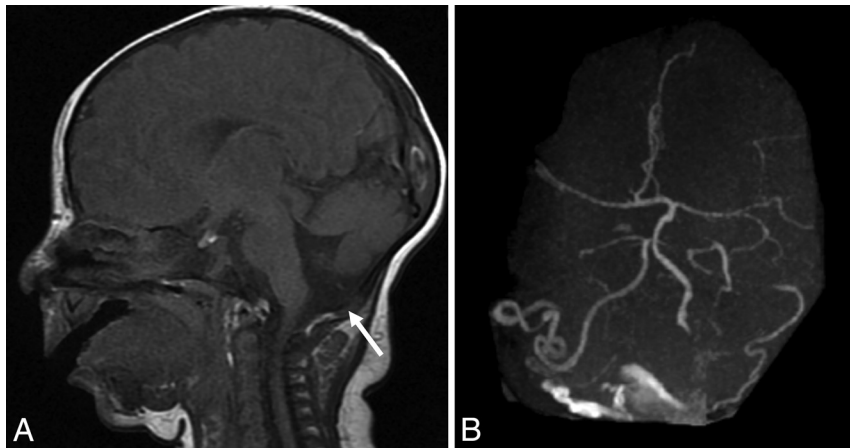


**FIG 18. PHACES syndrome.** Sagittal T1WI (A) shows a patient with a posterior fossa cystic malformation (arrow). Oblique coronal intracranial MIP MRA (B) shows absence of right ICA and left vertebral artery.

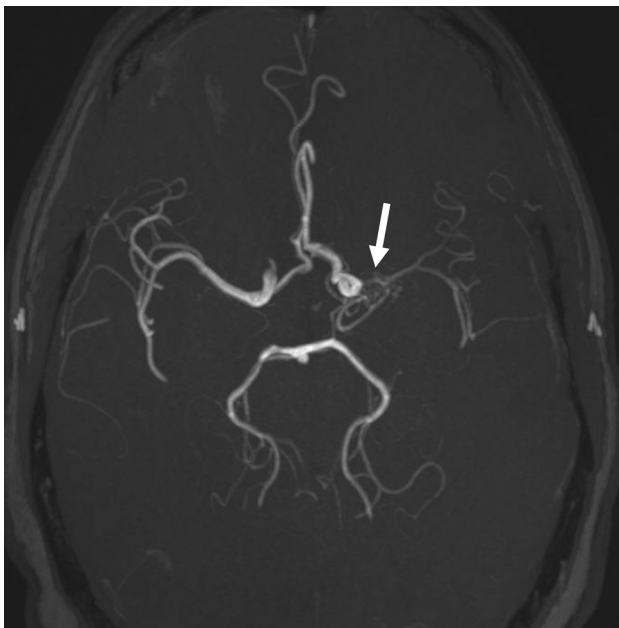


**FIG 19. Rete mirabile or twig-like.** Axial arterial MRA MIP indicates an absent left MCA with multiple vascular channels without distal ICA stenosis (arrow).

focal arteriopathy / poststroke (REF). The patient may be asymptomatic, though in some cases, it may be related to a hemorrhagic or ischemic stroke. Conventional cerebral angiography is recommended for diagnosis, and treatment is usually conservative.<sup>51</sup>

### Dilation

**Aneurysm.** The prevalence of intracranial aneurysms is much lower in children than in adults. Pediatric intracranial aneurysms include saccular, posttraumatic (dissecting aneurysms), infectious, and genetically related, such as PHACE, ACTA-2, polycystic kidney disease, HHT, hereditary angiopathy with nephropathy, aneurysms, and muscle cramps (HANAC) syndrome, Tuberous sclerosis, Ehlers-Danlos, and

Marfan, and Klippel-Trenaunay syndromes, among others. Hereditary aneurysms in children and young adults range from 5% to 20% and <5% of prepubertal patients. Children are more likely to have giant aneurysms (>2.5 cm) than multiple aneurysms. The patient is usually asymptomatic or can present with headaches, loss of consciousness, seizures, focal deficits, and vision changes. Aneurysms of >3 mm or symptomatic are usually treated, and mycotic aneurysms may regress with antibiotic therapy. When indicated, imaging follow-up is usually with MRA at baseline, 6 months after baseline, and annually for 5 years, followed by every 3–5 years for life.<sup>3,52,53</sup>

### Intracranial Arterial Dissection and Pseudoaneurysm

It is a rare entity present in childhood usually related to head trauma, extension of cervical arterial dissection, intracranial infections, mainly involving the internal carotid and middle cerebral arteries.<sup>54</sup> Intracranial pseudoaneurysms are rare, accounting for <1% of all intracranial aneurysms, and are unstable lesions without a complete aneurysm wall structure, corresponding to an organizing hematoma and fibrosis outside the true lumen instead of normal vascular elements (Fig 20). They can present with seizures, focal neurologic deficits and intracerebral hematoma, and the treatment may be craniotomy or endovascular procedures.<sup>55</sup>

### Fabry Disease

Fabry disease is a lysosomal storage disorder that affects multiple organs and is associated with mutations in the *GLA* gene, which produces the enzyme  $\alpha$ -galactosidase A. Clinical signs might vary and rely on the particular gene deficiency and level of residual enzyme activity, with several phenotypes affecting both males and heterozygous females. The main neuroimaging findings are stroke (with a predilection for females and young subjects), white matter hyperintensities (the most common neuroimage finding observed in up to 80% of patients), vascular dolichoectasia (the vertebrobasilar system is commonly affected), and other vessel abnormalities such as elongation, tortuosity, and focal

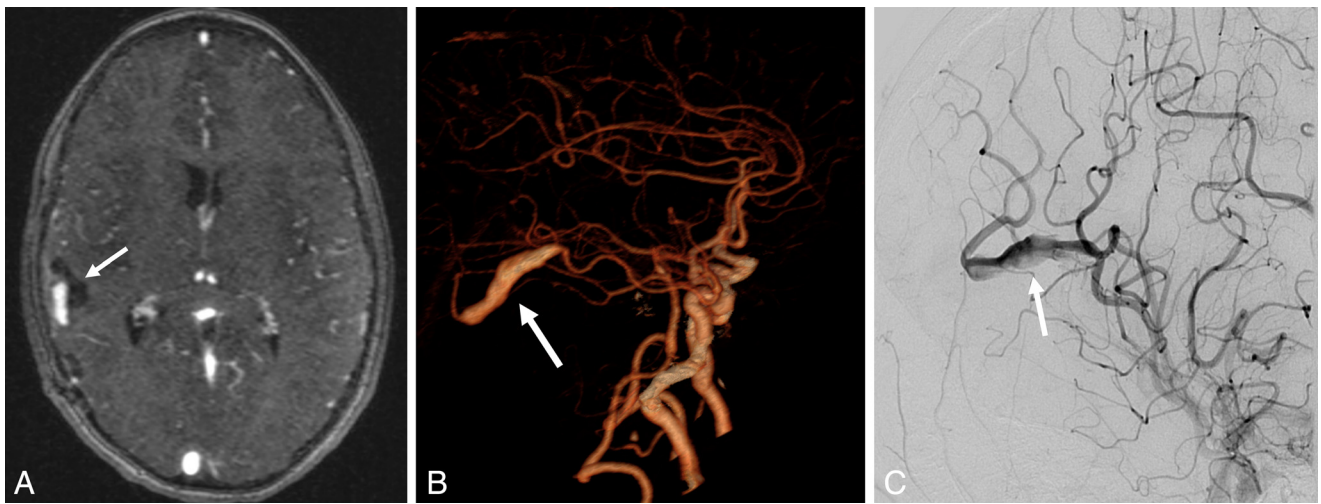


**FIG 20.** Pseudoaneurysm after surgical resection of a brain tumor. Axial venous MRA (A), 3D reconstruction from arterial angiography (B), and arterial intracranial angiography show an elongated and dilated vascular structure (B and C) adjacent to the surgical cavity (arrow).

aneurysmal dilation. The pulvinar sign is characterized by unilateral or bilateral hyperintensity of the thalamic pulvinar on unenhanced T1-weighted brain MRI, present in only 3% of patients, mostly observed in male patients with severe renal involvement. Due to its low incidence and specificity, it should no longer be recognized as a neuroradiologic classic finding of Fabry disease.<sup>56</sup>

### Stenosis

**Moyamoya Pattern.** The Moyamoya pattern can present as primary idiopathic Moyamoya disease (MMD) or secondary causes, such as NF1, Down syndrome, and sickle cell anemia, also known as Moyamoya syndrome. MMD is frequently seen in East Asian populations, more common in Japan and Korea, and is correlated with a polymorphism in the Ring Finger Protein 213 (*RNF213*) gene at chromosome 17q25.3, which is associated with an early onset and severe form of MMD, though the spectrum of *RNF213* variant mutation includes non-MMD disorders such as intracranial atherosclerosis and systemic vasculopathy.<sup>57</sup> MMD has a bimodal peak age of 5–10 years and later during the fourth decade and clinically presents in childhood as a recurrent TIA, while hemorrhage is rare, unlike in adults. The typical pattern of MMD is a progressive narrowing of the terminal internal carotid and proximal anterior and middle cerebral arteries, rarely involving the posterior circulation, which is followed by a development of fragile collaterals, which cause the “puff-of-smoke” appearance on angiography. The slow flow related to leptomeningeal anastomosis presents as a hyperintense signal in the cortical sulcus on FLAIR, termed the “ivy sign.” On postcontrast MR images it demonstrate corresponding vascular enhancement (Fig 21). Cerebral perfusion, including DSC-MR and ASL, can be used to evaluate acute stroke areas and quantify revascularization therapies.<sup>58,59</sup> The vessel narrowing is graded

according to the Suzuki classification (Table 2), and management, despite treating the main causes of secondary disease, is mainly by indirect bypass, such as encephaloduroarteriomyosynangiosis, which consists of the rerouting the artery, dura mater, and a layer of muscle (usually the temporalis muscle) in the synangiosis, bypassing the narrowed vessels of Moyamoya, or encephaloduroarteriosynangiosis, which involves attaching the superficial temporal artery and dura mater to the brain surface without the use of a muscle graft or by direct bypass of the superficial temporal artery with the MCA, which is more often used in adults. Successful revascularization is characterized by a reduction of the basal collateral and improvement of MCA branches.<sup>60,61</sup>

### Reversible Cerebral Vasoconstriction Syndrome and Posterior Reversible Encephalopathy Syndrome

Reversible cerebral vasoconstriction syndrome (RCVS), or Call-Flammer Syndrome, is a transient intracranial vasculopathy characterized by reversible, multifocal cerebral artery vasoconstriction associated with thunderclap headaches and/or focal neurologic deficits. It is more common in adults, but it has been reported in pediatric patients, with a male predominance. The reported triggers in children are trauma, exercise, water to the face, hypertension, and medication. In addition to vasoconstriction, it can be associated with subarachnoid and/or intraparenchymal hemorrhage and a reduction in CBF on ASL. RCVS may be associated with posterior reversible encephalopathy, which is not always posterior or reversible, and presents with headache, encephalopathy, and seizures related to high blood pressure. It is characterized by confluent subcortical T2/FLAIR-hyperintense white matter on MRI or hypodense white matter on CT, most commonly in the parietooccipital lobes, followed by the frontal lobe and vasoconstrictions (Fig 22), which may complicate ischemia and hemorrhage.<sup>63,64</sup> RCVS is a reversible syndrome, and

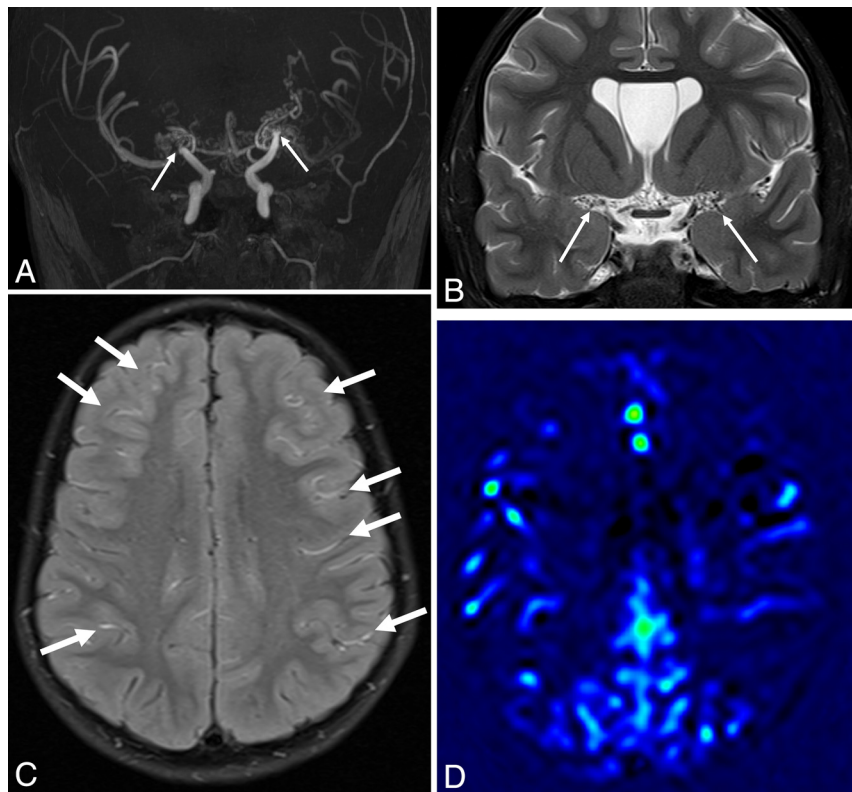


**FIG 21. Moyamoya pattern.** Coronal MIP MRA (A) shows narrowing of the bilateral distal ICAs and proximal MCAs with secondary collateral vessels in the Sylvian fissure on coronal T2WI (B). Axial FLAIR MRI (C) indicates hypersignal in the frontoparietal sulci, so-called ivy sign (arrows). Brain ASL perfusion (D) demonstrates bilateral CBF reduction in the anterior and middle cerebral arteries circulation.

**Table 2: Suzuki classification of Moyamoya disease<sup>62</sup>**

Stage	Definition
I	Narrowing of carotid fork
II	Initiation of the Moyamoya: dilation of ACA and MCA, initial Moyamoya blush
III	Intensification of the Moyamoya: stenosis/occlusion of ACA and MCA, increased Moyamoya blush
IV	Minimization of the Moyamoya: progressive stenosis/occlusion of ICA reaching PCA origin and reduction of Moyamoya blush
V	Reduction of the Moyamoya: occlusion of ICA, ACA, and MCA, and collateral supply from ECA
VI	Disappearance of the Moyamoya: no blood supply from ICA; intracranial blood supply made exclusively by ECA and vertebral artery.

**Note:**—ECA indicates external carotid artery; ACA, anterior cerebral artery; PCA, posterior cerebral artery.

the recommended imaging follow-up at 3 months usually shows resolution of vasoconstrictions. Additionally, an improvement in CBF on ASL is expected on follow up, even though in certain instances, an enhanced perfusion may be seen, which may be connected to therapy-induced reperfusion hyperemia.<sup>65</sup>

### Vasculitis

Vasculitis is a heterogeneous group of diseases characterized by blood vessel wall inflammation, which may develop as a primary or secondary condition. The European League against Rheumatism recently proposed new consensus criteria for the classification of childhood vasculitis according to the vessel involved: 1) predominantly large-sized vessel vasculitis (Takayasu arteritis); 2) predominantly medium-sized

vessel vasculitis (childhood polyarteritis nodosa, cutaneous polyarteritis, and Kawasaki disease); 3) predominantly small-vessel vasculitis subdivided into 2 groups: granulomatous (Wegener granulomatosis and Churg-Strauss syndrome) and nongranulomatous (microscopic polyangiitis, Henoch-Schönlein purpura, isolated cutaneous leukocytoclastic vasculitis, hypocomplementic urticarial vasculitis urticarial vasculitis), and 4) other vasculitis (Behçet disease, vasculitis secondary to infection, including hepatitis B-associated polyarteritis nodosa, malignancies, and drugs, such as hypersensitivity vasculitis, vasculitis associated with connective tissue diseases, isolated vasculitis of the CNS, Cogan syndrome, and unclassified).<sup>66</sup> Clinically, patients may present with intractable seizures, paresis, cognitive deficits, and/or cranial nerve deficits. The imaging work-up consists of a

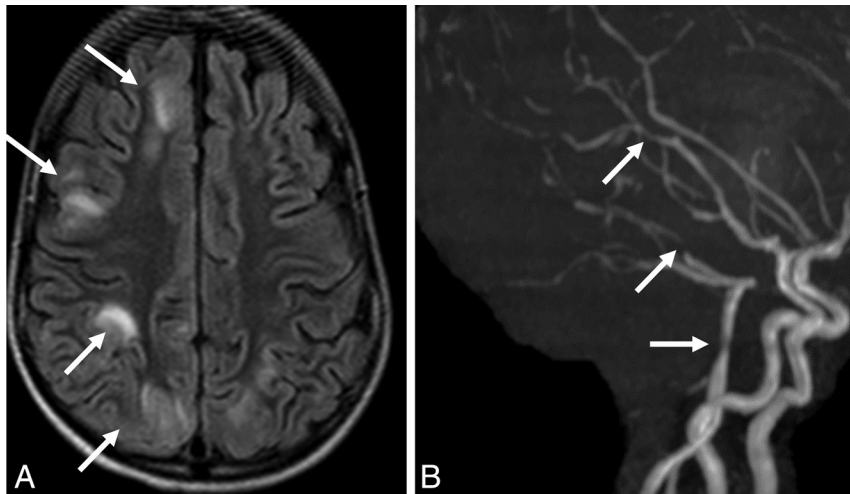


**FIG 22.** RCVS and posterior reversible encephalopathy syndromes. Girl, 8 years of age, with a recent history of transplantation. Axial FLAIR MRI (A) shows subcortical frontoparietal high signal (arrows) without DWI restriction (not shown), compatible with vasogenic edema. Oblique sagittal MRA (B) demonstrates irregularities and multiple focal narrowing at the middle and posterior arterial branches and basilar artery, related to vasoconstriction (arrows).

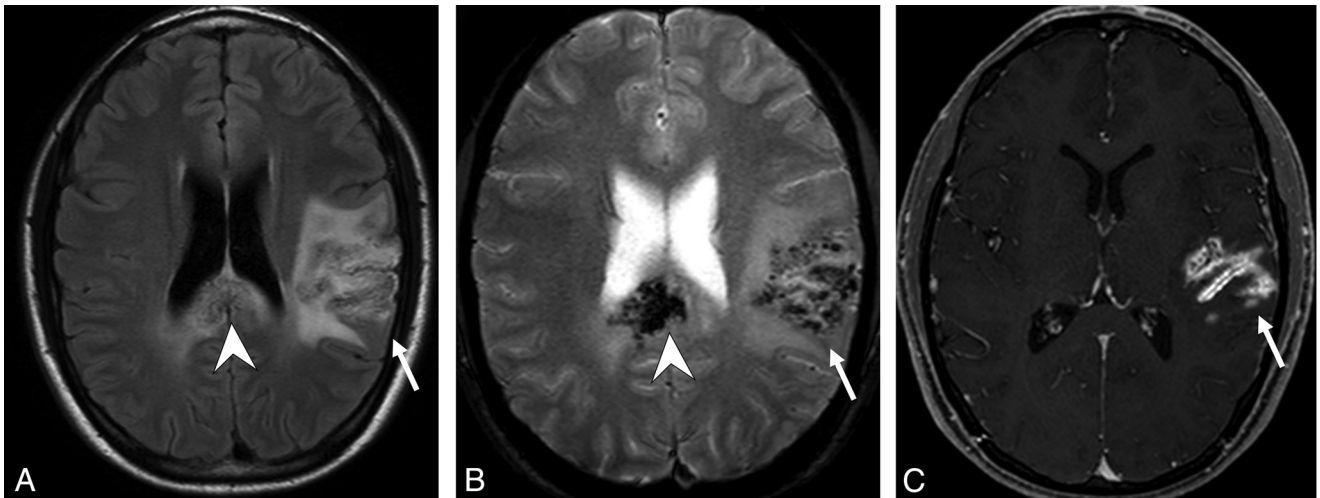


**FIG 23.** Patient with lymphocytic primary CNS angiitis confirmed by brain biopsy. Axial FLAIR MRI (A) shows high signal intensity in the left parietal lobe (arrow) and splenium corpus callosum (arrowhead). Axial gradient-recalled echo image (B) demonstrates bleeding foci in the left parietal lobe (arrow) and splenium corpus callosum (arrowhead). Axial T1 postcontrast MRI (C) indicates gyral enhancement (arrow).

brain MRI with MR angiography/venography and DSA. The last one is the criterion standard for the diagnosis of these conditions. Imaging findings include vessel narrowing, beading, multiple dilatations, aneurysms, avascular mass lesions, concentric thickening with enhancement and some studies may still be normal.

For primary CNS angiitis (Fig 23), the most common vascular involvement is unilateral and proximal, involving the anterior circulation with multifocal parenchymal lesions within a lenticulostriate distribution. Biopsy remains the criterion standard for diagnosis.<sup>67</sup> Some vasculitis cases may present as transient cerebral arteriopathy or focal cerebral arteriopathy, including varicella zoster virus infection, which is one of the most common causes of arterial ischemic stroke in children (Fig 24). The imaging findings are

unilateral focal or segmental stenosis or occlusion involving the distal part of the internal carotid and the initial segments and branches of the ACA (anterior cerebral artery) and/or MCA with enhancement of the affected arterial segment demonstrated on vessel wall imaging.<sup>68</sup> Transient cerebral arteriopathy is usually treated with corticosteroids, which may be associated with other medications depending on the cause, and the progressive vascular findings have triple the risk of recurrent ischemic events.<sup>69</sup>

#### **Small Vessel Vasculopathy**

**Deficiency of Adenosine Deaminase 2.** Deficiency of adenosine deaminase 2 is an autosomal recessive disorder of the ADA2 gene (previously known as *CECR1*), which is located

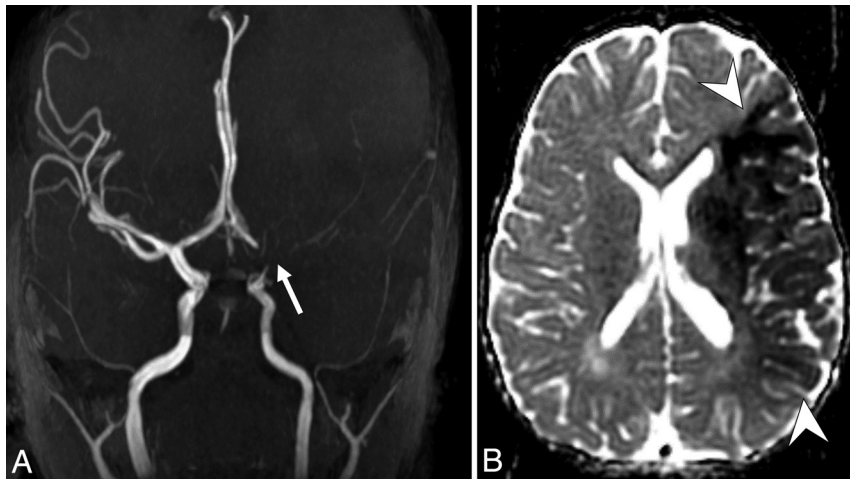


**FIG 24. Varicella-zoster vasculopathy. Coronal MIP MRA (A) demonstrates occlusion of the MCA and left proximal segment of the ICA (arrow). Axial ADC map (B) shows an area of acute cerebral ischemia (arrowheads).**

at 22q11.1 and has a wide clinical spectrum from cutaneous findings, such as polyarteritis nodosa-like vasculopathy, to pure hematologic disorders without vasculopathy. CNS findings were reported in almost 75% of patients, characterized by lacunar infarctions and hemorrhages usually located in the nucleocapsular, mesencephalic, and thalamic regions, secondary to small- and medium-sized vessel vasculopathy, in some cases with normal findings on arteriography. Aneurysms may be associated with this syndrome, as well as eccentric vessel wall thickening and enhancement, especially at the origin of the brainstem perforators. The last one can lead to progressive arterial stenosis. The early diagnosis and management of these pathologies with tumor necrosis factor inhibitors leads to remission and prevents future neurologic events.<sup>70</sup>

#### **Vasculopathy Secondary to Systemic Lupus Erythematosus**

Pediatric systemic lupus erythematosus (SLE) affects 3.3–8.8 per 100,000 children, and 20% of patients with lupus are diagnosed in childhood. CNS SLE involvement or neuropsychiatric lupus erythematosus frequently occurs in pediatric lupus. SLE vasculopathy predominantly affects arterioles and capillaries, presenting with vessel tortuosity, endothelial proliferation, perivascular inflammation, gliosis, and 31% of patients with SLE had cerebral vasculitis. The imaging findings were T2WI hyperintense in the justacortical, deep, and periventricular white matter, lacunar infarction, brain atrophy, intracranial hemorrhage such as microhemorrhage, and SAH. Although rare, when major intracranial hemorrhage is present, it is associated with high mortality. Large infarctions are reported in approximately 10%–15% of patients, with a mean age of 35–40 years. Vessel wall imaging may reveal concentric wall thickening.<sup>71,72</sup>

#### **CONCLUSIONS**

Intracranial vascular diseases in childhood are a wide group of pathologies and a clinical challenge because of the many

signs and symptoms in addition to asymptomatic pathologies “to” and a clinical challenge due to its variable signs and symptoms, or even the absence of them to look for in some pathologies, and on imaging, these diseases can be classified through shunting and nonshunting pathologies and later by vessel morphology.

#### **REFERENCES**

1. Sabayan B, Lineback C, Viswanathan A, et al. Central nervous system vascular malformations: a clinical review. *Ann Clin Transl Neurol Wiley Neurol* 2021;8:504–22. 10.1002/acn3.51277
2. Cruz JP, Gandolfo C, Geibprasert S, et al. Pediatric vascular malformations of the brain: concepts and classifications, diagnosis and endovascular treatment. *Pediatric Neuroradiology*. Berlin Heidelberg: Springer-Verlag; 2015:1–36.
3. Montaser A, Smith ER. Intracranial vascular abnormalities in children. *Pediatr Clin North Am* 2021;68:825–43. 10.1016/j.pcl.2021.04.010
4. Lawton MT, Rutledge WC, Kim H, et al. Brain arteriovenous malformations. *Nat Rev Dis Primers* 2015;1:15008. 10.1038/nrdp.2015.8
5. Geibprasert S, Pongpech S, Jiarakongmun P, et al. Radiologic assessment of brain arteriovenous malformations: what clinicians need to know. *Radiographics* 2010;30:483–501. 10.1148/rg.302095728
6. Ansari SA, Schnell S, Carroll T, et al. Intracranial 4D flow MRI: toward individualized assessment of arteriovenous malformation hemodynamics and treatment-induced changes. *AJNR Am J Neuroradiol* 2013;34:1922–28. 10.3174/ajnr.A3537
7. Kim DJ, Krings T. Whole-brain perfusion CT patterns of brain arteriovenous malformations: a pilot study in 18 patients. *AJNR Am J Neuroradiol* 2011;32:2061–66. 10.3174/ajnr.A2659
8. Blauwblomme T, Naggara O, Brunelle F, et al. Arterial spin labeling magnetic resonance imaging: toward noninvasive diagnosis and follow-up of pediatric brain arteriovenous malformations. *J Neurosurg Pediatr* 2015;15:451–58. 10.3171/2014.9.PEDS14194
9. Iutaka T, de Freitas MB, Omar SS, et al. Arterial spin labeling: techniques, clinical applications, and interpretation. *Radiographics* 2023;43:e220088. 10.1148/rg.220088

10. Spetzler RF, Martin NA. A proposed grading system for arteriovenous malformations. *J Neurosurg* 1986;65:476–83. 10.3171/jns.1986.65.4.0476
11. Yu J, Lv X, Li Y, et al. Therapeutic progress in pediatric intracranial dural arteriovenous shunts: a review. *Interv Neuroradiol* 2016;22:548–56. 10.1177/1591019916653254
12. Lv X, Jiang C, Wang J. Pediatric intracranial arteriovenous shunts: advances in diagnosis and treatment. *Eur J Paediatr Neurol* 2020;25:29–39. 10.1016/j.ejpn.2019.12.025
13. Díaz C, Auctores Publishing LLC, eds. Endovascular treatment of intracranial pial arteriovenous fistula in paediatric patient. *JNNS* 2021;8:01–05. 10.31579/2578-8868/167
14. Sammoud S, Hammami N, Turki D, et al. Acquired pial arteriovenous fistula secondary to cerebral cortical vein thrombosis: a case report and review of the literature. *Neuroradiol J* 2022;35:515–19. 10.1177/19714009211049080
15. Walcott BP, Smith ER, Scott MR, et al. Pial arteriovenous fistulae in pediatric patients: associated syndromes and treatment outcome. *J Neurointerv Surg* 2013;5:10–14. 10.1136/neurintsurg-2011-010168
16. Paramasivam S, Toma N, Niimi Y, et al. Development, clinical presentation and endovascular management of congenital intracranial pial arteriovenous fistulas. *J Neurointerv Surg* 2013;5:184–90. 10.1136/neurintsurg-2011-010241
17. Mortazavi MM, Griessenauer CJ, Foreman P, et al. Vein of Galen aneurysmal malformations: Critical analysis of the literature with proposal of a new classification system. *J Neurosurg Pediatr* 2013;12:293–306. 10.3171/2013.5.PEDS12587
18. Saliou G, Vranka I, Teglas J, et al. Pseudofeeders on fetal magnetic resonance imaging predict outcome in vein of Galen malformations. *Ann Neurol* 2017;81(2):278–286.
19. Arko L, Lambrych M, Zurakowski D, Orbach DB. Fetal and Neonatal MRI Predictors of Aggressive Early Clinical Course in Vein of Galen Malformation. *American Journal of Neuroradiology* 2020;4181(6):1105–1111.
20. Saliou G, Dirks P, Sacho RH, Chen L, terBrugge K, Krings T. Decreased Superior Sagittal Sinus Diameter and Jugular Bulb Narrowing Are Associated with Poor Clinical Outcome in Vein of Galen Arteriovenous Malformation. *American Journal of Neuroradiology* 2016;37(7):1354–1358.
21. Shigematsu T, Bazil MJ, Fifi JT, Berenstein A. Fine, Vascular Network Formation in Patients with Vein of Galen Aneurysmal Malformation. *American Journal of Neuroradiology* 2022; 43(10):1481–1487.
22. Berenstein A, Paramasivam S, Sorscher M, et al. Vein of Galen aneurysmal malformation: advances in management and endovascular treatment. *Clin Neurosurg* 2019;84:469–78. 10.1093/neuros/nyy100
23. Puerta P, Guillén A, Muchart J, et al. Cerebral proliferative angiopathy in a child. *Pediatr Neurosurg* 2017;52:214–16. 10.1159/000459629
24. Vilela P. (2019). Cranial Vessel Embryology and Imaging Anatomy. In *Clinical Neuroradiology* (pp. 95–135). Springer International Publishing. 10.1007/978-3-319-68536-6\_20
25. Sheppard SE, Sanders VR, Srinivasan A, et al. Cerebrofacial vascular metamerism syndrome is caused by somatic pathogenic variants in PIK3CA. *Cold Spring Harb Mol Case Stud* 2021;7:00614710.1101/mcs.a006147
26. ten Broek RW, Eijkelenboom A, van der Vleuten CJ, et al. Comprehensive molecular and clinicopathological analysis of vascular malformations: a study of 319 cases. *Genes Chromosomes Cancer* 2019;58:541–50. 10.1002/gcc.22739
27. O’Loughlin L, Groves ML, Miller NR, et al. Cerebrofacial arteriovenous metamerism syndrome (CAMS): a spectrum disorder of craniofacial vascular malformations. *Childs Nerv Syst* 2017;33:513–16. 10.1007/s00381-016-3277-x
28. Hetts SW, Shieh JT, Ohliger MA, et al. Hereditary hemorrhagic telangiectasia: the convergence of genotype, phenotype, and imaging in modern diagnosis and management of a multi-system disease. *Radiology* 2021;300:17–30. 10.1148/radiol.2021203487
29. Ring NY, Latif MA, Hafezi-Nejad N, et al. Prevalence of and factors associated with arterial aneurysms in patients with hereditary hemorrhagic telangiectasia: 17-year retrospective series of 418 patients. *J Vasc Interv Radiol* 2021;32:1661–69. 10.1016/j.jvir.2021.08.018
30. Krings T, Kim H, Power S, et al. Brain Vascular Malformation Consortium HHT Investigator Group. Neurovascular manifestations in hereditary hemorrhagic telangiectasia: imaging features and genotype-phenotype correlations. *AJNR Am J Neuroradiol* 2015;36:863–70. 10.3174/ajnr.A4210
31. Brinjikji W, Mark IT, Silvera VM, et al. Cervicofacial venous malformations are associated with intracranial developmental venous anomalies and dural venous sinus abnormalities. *AJNR Am J Neuroradiol* 2020;41:1209–14. 10.3174/ajnr.A6617
32. Brinjikji W, Nicholson P, Hilditch CA, et al. Cerebrofacial venous metamerism syndrome—spectrum of imaging findings. *Neuroradiology* 2020;62:417–25. 10.1007/s00234-020-02362-7
33. Brinjikji W, Hilditch CA, Tsang AC, et al. Facial venous malformations are associated with cerebral developmental venous anomalies. *AJNR Am J Neuroradiol* 2018;39:2103–07. 10.3174/ajnr.A5811
34. Geraldo AF, Messina SS, Tortora D, et al. Neonatal developmental venous anomalies: clinicoradiologic characterization and follow-up. *AJNR Am J Neuroradiol* 2020; 41:2370–76. 10.3174/ajnr.A6829
35. Tan ZG, Zhou Q, Cui Y, et al. Extra-axial isolated cerebral varix misdiagnosed as convexity meningioma: a case report and review of literatures. *Medicine (Baltimore)* 2016;95: e4047. 10.1097/MD.0000000000004047
36. Ceylan AH, Nascene DR, Huang H, et al. Torcular pseudomass in newborns and its association with delivery: follow up or leave it alone? *Neuroradiology* 2022;64:2069–76. 10.1007/s00234-022-02981-2
37. Merello E, Pavanello M, Consales A, et al. Genetic screening of pediatric cavernous malformations. *J Mol Neurosci* 2016;60:232–38. 10.1007/s12031-016-0806-8
38. Zabramski JM, Wascher TM, Spetzler RF, Johnson B, Golfinos J, Drayer BP, Brown B, Rigamonti D, Brown G. The natural history of familial cavernous malformations: results of an ongoing study. *J Neurosurg* 1999 Mar;80(3):422–32. 10.3171/jns.1994.80.3.0422
39. D’Arco F, Alves CA, Raybaud C, et al. Expanding the distinctive neuroimaging phenotype of ACTA2 mutations. *AJNR Am J Neuroradiol* 2018;39:2126–31. 10.3174/ajnr.A5823
40. Manara R, D’Agata L, Rocco MC, et al; Menkes Working Group in the Italian Neuroimaging Network for Rare Diseases. Neuroimaging changes in menkes disease, part 1.

- AJNR Am J Neuroradiol* 2017;38:1850–57. 10.3174/ajnr.A5186
41. Manara R, Rocco MC, D’agata L, et al; Menkes Working Group in the Italian Neuroimaging Network for Rare Diseases. **Neuroimaging changes in menkes disease, Part 2: menkes working group in the Italian neuroimaging network for rare diseases.** *AJNR Am J Neuroradiol* 2017;38:1858–65. 10.3174/ajnr.A5192
  42. Parlapiano G, Di Lorenzo F, Salehi LB, et al. **Neurovascular manifestations in connective tissue diseases: the case of Marfan syndrome.** *Mech Ageing Dev* 2020;191:111346. 10.1016/j.mad.2020.111346
  43. Zilocchi M, Macedo TA, Oderich GS, et al. **Vascular Ehlers-Danlos syndrome: Imaging findings.** *AJR Am J Roentgenol* 2007;189:712–19. 10.2214/AJR.07.2370
  44. Rodrigues VJ, Elsayed S, Loeys BL, et al. **Neuroradiologic manifestations of Loeys-Dietz syndrome type 1.** *AJNR Am J Neuroradiol* 2009;30:1614–19. 10.3174/ajnr.A1651
  45. Spinardi L, Vornetti G, de Martino S, et al. **Intracranial arterial tortuosity in marfan syndrome and loeys-dietz syndrome: tortuosity index evaluation is useful in the differential diagnosis.** *AJNR Am J Neuroradiol* 2020;41:1916–22. 10.3174/ajnr.A6732
  46. Oderich GS, Sullivan TM, Bower TC, et al. **Vascular abnormalities in patients with neurofibromatosis syndrome type I: clinical spectrum, management, and results.** *J Vasc Surg Mosby Inc* 2007;46:475–84. 10.1016/j.jvs.2007.03.055
  47. Kaas B, Huisman TA, Tekes A, et al. **Spectrum and prevalence of vasculopathy in pediatric neurofibromatosis type 1.** *J Child Neurol* 2013;28:561–69. 10.1177/0883073812448531
  48. Heyer GL, Dowling MM, Licht DJ, et al. **The Cerebral Vasculopathy of PHACES Syndrome.** *Stroke* 2008;39(2):308–316.
  49. Garzon MC, Epstein LG, Heyer GL, et al. **PHACE syndrome: consensus-derived diagnosis and care recommendations.** *J Pediatr* 2016;178:24–33.e2. 10.1016/j.jpeds.2016.07.054
  50. Kossorotoff M, Grévent D, Roux C-J, Brunelle F. **Development of Collateral Vessels after Anterior Circulation Large Vessel Occlusion in Pediatric Arterial Ischemic Stroke Relates to Stroke Etiology: A Longitudinal Study.** *American Journal of Neuroradiology* 2024;45(3):271–276.
  51. Seo BS, Lee YS, Lee HG, et al. **Clinical and radiological features of patients with aplastic or twiglike middle cerebral arteries.** *Neurosurgery* 2012;70:1472–80; discussion 1480. 10.1227/NEU.0b013e318246a510
  52. Gross BA, Smith ER, Scott RM, et al. **Intracranial aneurysms in the youngest patients: characteristics and treatment challenges.** *Pediatr Neurosurg* 2015;50:18–25. 10.1159/000370161
  53. Garg K, Singh PK, Sharma BS, et al. **Pediatric intracranial aneurysms: our experience and review of literature.** *Childs Nerv Syst* 2014;30:873–83. 10.1007/s00381-013-2336-9
  54. Stence N, V, Fenton LZ, Goldenberg NA, et al. **Craniocervical arterial dissection in children: diagnosis and treatment.** *Curr Treat Options Neurol* 2011;13:636–48. 10.1007/s11940-011-0149-2
  55. Chen R, Zhang S, Guo R, et al. **Pediatric intracranial pseudoaneurysms: a report of 15 cases and review of the literature.** *World Neurosurg* 2018;116:e951–59. 10.1016/j.wneu.2018.05.140
  56. Coccozza S, Russo C, Pontillo G, et al. **Neuroimaging in Fabry disease: current knowledge and future directions.** *Insights Imaging* 2018;9:1077–88. 10.1007/s13244-018-0664-8
  57. Bang OY, Chung JW, Kim DH, et al. **Moyamoya disease and spectrums of RNF213 vasculopathy.** *Transl Stroke Res* 2020;11:580–89. 10.1007/s12975-019-00743-6
  58. Li J, Jin M, Sun X, et al. **Imaging of Moyamoya disease and Moyamoya syndrome: current status.** *J Comput Assist Tomogr* 2019;43:257–63. 10.1097/RCT.0000000000000834
  59. Soun JE, Song JW, Romero JM, et al. **Central nervous system vasculopathies.** *Radiology Clin North Am* 2019;57:1117–31. 10.1016/j.rcl.2019.07.005
  60. Wen LZ, Han C, Zhao F, et al. **Collateral circulation in Moyamoya disease a new grading system.** *Stroke* 2019;50:2708–15. 10.1161/STROKEAHA.119.024487
  61. Acker G, Fekonja L, Vajkoczy P. **Surgical management of Moyamoya disease.** *Stroke* 2018;49:476–82. 10.1161/STROKEAHA.117.018563
  62. Suzuki J, Takaku A. **Cerebrovascular “Moyamoya” Disease.** *Arch Neurol* 1969;20:288–99. 10.1001/archneur.1969.00480090076012
  63. Chen T-H. **Childhood posterior reversible encephalopathy syndrome: clinicoradiological characteristics, managements, and outcome.** *Front Pediatr* 2020;8:585. 10.3389/fped.2020.00585
  64. Coffino SW, Fryer RH. **Reversible cerebral vasoconstriction syndrome in pediatrics: a case series and review.** *J Child Neurol* 2017;32:614–23. 10.1177/0883073817696817
  65. Kayfan S, Sharifi A, Xie S, et al. **MRA and ASL perfusion findings in pediatric reversible cerebral vasoconstriction syndrome.** *Radiol Case Rep* 2019;14:832–36. 10.1016/j.radcr.2019.04.010
  66. Iannetti L, Zito R, Bruschi S, et al. **Recent understanding on diagnosis and management of central nervous system vasculitis in children.** *Clin Dev Immunol* 2012;2012:698327–29. 10.1155/2012/698327
  67. Aviv RI, Benseler SM, Silverman ED, et al. **MR imaging and angiography of primary CNS vasculitis of childhood.** *AJNR Am J Neuroradiol* 2006;27:192–99.
  68. Younger DS, Coyle PK. **Central nervous system vasculitis due to infection.** *Neurol Clin* 2019;37:441–63. 10.1016/j.ncl.2019.01.002
  69. Fullerton HJ, Stence N, Hills NK, et al; VIPS Investigators. **Focal cerebral arteriopathy of childhood: novel severity score and natural history.** *Stroke* 2018;49:2590–96. 10.1161/STROKEAHA.118.021556
  70. Geraldo AF, Caorsi R, Tortora D, et al. **Widening the neuroimaging features of adenosine deaminase 2 deficiency.** *AJNR Am J Neuroradiol* 2021;42:975–79. 10.3174/ajnr.A7019
  71. Ide S, Kakeda S, Miyata M, et al. **Intracranial vessel wall lesions in patients with systematic lupus erythematosus.** *J Magn Reson Imaging* 2018;48:1237–46. 10.1002/jmri.25966
  72. Ota Y, Srinivasan A, Capizzano AA, et al. **Central nervous system systemic lupus erythematosus: pathophysiologic, clinical, and imaging features.** *Radiographics* 2022;42:212–32. 10.1148/rg.210045